

9260

NACA TN 2945

0066173



TECH LIBRARY KAFB, NM

# NATIONAL ADVISORY COMMITTEE FOR AERONAUTICS

TECHNICAL NOTE 2945

THE CREEP OF SINGLE CRYSTALS OF ALUMINUM

By R. D. Johnson, F. R. Shober, and A. D. Schwope

Battelle Memorial Institute



Washington

May 1953

AFMDC  
TECHNICAL LIBRARY  
AFL 2811



## TECHNICAL NOTE 2945

## THE CREEP OF SINGLE CRYSTALS OF ALUMINUM

By R. D. Johnson, F. R. Shober, and A. D. Schwope

## SUMMARY

This report covers the work carried out in a fundamental investigation of creep in metals and, in particular, the creep of single crystals of aluminum in the temperature range from room temperature to 400° F.

The experimental results from the creep tests are in good agreement with the time dependence predicted by the Andrade relation over a limited time interval, especially at resolved shear stresses above 200 psi, when analyzed in terms of shear strain rates. This is in agreement with the relation between strain rate and time for polycrystals, thus providing a link between the behavior of single-crystal and polycrystalline materials. The variation of the creep rate with shear stress and temperature is more complex.

In tensile and constant-load-rate tests of these single crystals the stress required to produce a given strain decreased with increasing temperature, as expected, except in cases where the orientation of the crystals was such as to induce duplex slip early in the plastic deformation. In some cases the orientation of the crystal seemed to affect the shape of the curve of shear stress against shear strain.

A study of the strain markings on the specimens indicated that slip was one of the mechanisms, and probably the predominant one, in deformation by a constant-load creep test and by an increasing-load tensile test.

## INTRODUCTION

This investigation was conducted to obtain reliable creep data under well-controlled experimental conditions, in order to substantiate or refute the currently popular theories of creep (ref. 1), in particular, transient creep, and to lend support to a new theory if the present ones fail. The experiments have been designed to attempt to obtain supplementary evidence with regard to the type or mechanism of deformation on a microscopic as well as a macroscopic scale, since it is believed that the mathematical formulation of the phenomena will be forthcoming when the mechanism of creep is better understood.

Single-crystal specimens of high-purity (99.99+ percent) aluminum have been used to attempt to reduce the number of obvious variables under consideration to a minimum. The effects of temperature, stress, and time on the creep rate have been observed. The temperature range investigated was from room temperature to 400° F. The same resolved-shear-stress levels were used at the various temperatures. The lowest resolved shear stress used, 200 psi, was the lowest shear stress which produced measurable creep at room temperature, since it has been found that the single crystals will not creep at room temperature unless the resolved shear stress is greater than the critical resolved shear stress by an order of magnitude (ref. 2). The highest resolved shear stress used, 400 psi, was dictated by the need to keep the strains low enough for the constant-load tests to approximate closely constant-stress tests, even at the higher temperatures, in order to facilitate interpretation. The creep data have been analyzed and the results discussed in view of existing creep theories.

The stress-strain curves of these single crystals of high-purity aluminum have been determined also by tensile tests and by constant-load-rate tests in the same temperature range in order to supplement the study of plastic deformation by creep with information to help evaluate the part that the crystal orientation, the differences in strain-hardening, and other hidden variables play in plastic deformation. These tests have stimulated ideas about the mechanism of plastic deformation by creep and have served as a basis for comparison with previously reported stress-strain curves for single crystals of aluminum (ref. 3).

This work was conducted at the Battelle Memorial Institute under the sponsorship and with the financial assistance of the National Advisory Committee for Aeronautics.

#### EQUIPMENT

##### Creep Units

Additional equipment has been constructed to facilitate the investigation of creep phenomena in metals. Six units have been designed and constructed and are now in use. All of the units were built incorporating those features which could be utilized to the greatest advantage in creep investigations. Three of these units were constructed with base plates and upper plates strong enough to withstand loads of 20,000 pounds, and the remaining three were made to withstand loads up to 10,000 pounds. These creep units can be used as direct-loading machines, or, with a slight modification which has been incorporated into two of the units, loading can be applied through a lever arm. All six units are large enough to test specimens of the standard 0.505-inch-diameter tensile type.

It is a simple matter to change from round specimens to sheet or even wire specimens, since only changing the adapters to hold the desired specimen is involved.

The direct-loading method can be used for stress levels up to 2,000 psi. The foremost advantage of this method is the ease with which axial loading can be accomplished. The direct load is applied through a fixed ball-seat arrangement, as described in reference 2. The direct-loading unit also has the advantage that it is small and compact as compared with the lever-arm machine.

The lever-arm attachments serve two purposes: (1) They convert the unit to one capable of producing higher loads on the specimen and (2) they make it possible to run creep tests in compression.

With the addition of the fifth and sixth creep units, it became necessary to move the entire setup to larger quarters, a constant-temperature room in which the temperature variation was maintained within  $\pm 1^{\circ}\text{C}$ . A portion of the creep equipment is shown in figure 1. The panel board in the center contains six Honeywell temperature controllers, one for each stand, and a six-point Honeywell recorder to record the signal put out by each capacitance strain gage.

#### Heating Method and Control Equipment for

##### Elevated-Temperature Tests

Electric resistance-type furnaces were used for heating in all elevated-temperature tests. The one-piece furnaces were wound so that each furnace contained three individual zones. Wiring in this way provided an excellent method of maintaining a more equal distribution of the temperature. The furnaces were 12 inches long, long enough to provide an adequate heating zone for the specimen and parts of the upper and lower adapters. Each zone was 4 inches long, which made it possible to have the entire gage length of the specimen in one zone. This prevented large fluctuations of temperature in the specimen and tended to minimize any temperature gradients in the specimen. In addition to the four one-piece furnaces, two split furnaces were constructed. These split furnaces have the advantage that they are easier to set up after the extensometer and specimen have been positioned correctly. They also permit shorter cooling periods, since they can be removed without removing the specimen.

The power to the furnace was regulated by a Variac connected to a Honeywell controller, recently installed in place of a Foxboro controller, which required an anticipator circuit to function properly. Calibration of the furnaces indicated that one thermocouple attached to the center of the gage section was sufficient for controlling and determining the

specimen temperature. Ordinarily, the thermocouple was insulated from the specimen by a thin sheet of mica to prevent any stray voltage pickup. The temperature of the specimen varied approximately  $\pm 1^{\circ}\text{C}$  during the tests.

#### Capacitance Strain Gage

A recording-type extensometer was designed for this work, since it was felt that it would be quite advantageous to be able to obtain the initial portion of the creep curve, which otherwise is lost because of the speed with which the initial extension of the specimen takes place. The convenience afforded by a continuously, automatically recorded strain-time curve also proved to be quite desirable.

An extensometer was designed with these particular ideas in mind. The result was an instrument which operates on the principle that the capacity of two parallel plates varies inversely with the distance between them. This method of strain measurement is then basically a method which measures the elongation of a specimen by measuring the change in capacitance of two parallel metal plates connected to a section of the specimen. It is not a new method, but in this particular application there were a number of difficulties which required modifications. The primary objectives were to develop an extensometer which had high sensitivity and freedom from drift and which was relatively simple to use.

A schematic diagram of the capacitance-strain-gage unit is shown in figure 2. The unit consists of two Armstrong-type oscillators and a voltage-adder circuit which adds voltages vectorially. Tuned circuits are coupled inductively to the oscillators and the voltage developed across these tank circuits is delivered to the voltage-adder circuit.

The frequency of the oscillators is adjustable and is set at a value just off the natural resonant frequency of the measuring tuned circuit. The amount of the off-tuning is such as to cause the measuring-tank circuit to operate on the most nearly linear portion of the resonant curve. Then this voltage change is sent to the voltage-adder circuit. The second oscillator is intended to furnish a balancing voltage for the voltage-adder circuit. The zeroing capacitor can be used then to rezero a recording instrument or can be calibrated in microinches and adjusted to balance for each reading.

The power supply used for the unit, which is actually a part of the unit, is represented schematically in figure 3. This power supply is of a standard type, with the exception of the addition of two rectifier tubes for greater stability and a two-section filter to minimize the ripple in the high voltage supply. Voltage regulators and bleeders are added to stabilize its output further. In the event that the line voltage is

extremely unstable, it is sometimes necessary to use a line regulator in conjunction with the power supply.

The performance of the extensometer is dependent upon two factors:

- (1) The size and shape of plate used for capacitor plates
- (2) The material from which the plates were constructed

The round capacitor plate was found to be the best shape. A plate diameter of  $1\frac{7}{8}$  inches was found to be large enough to make the edge effects negligible. The extensometer, pictured in figure 4, utilized arms to transmit the motion of the specimen to the capacitor plates outside of the furnace. The sensitivity is dependent upon the size of the plates and the distance between them. However, it can be varied by changing the 100-micromicrofarad variable condenser in the matched circuit (see fig. 2), in which case the sensitivity decreases as the total range is increased. Typical values from calibration curves indicate that, for a range of 2 percent, the sensitivity varies from 1.5 to 16 microinches per millivolt. When the range is increased to 10 percent, the sensitivity varies from 4 to 50 microinches per millivolt. The fact that the capacitance plates are outside the furnace is an advantage in that the unit need be calibrated only once for work at all temperatures, and the plates can be rezeroed to increase the total range of strain that can be measured with good sensitivity. However, the fact that the plates are outside of the furnace proves to be a disadvantage in that parts extending from the furnace are susceptible to errors due to their thermal expansion.

The output of the capacitance strain gage is fed into a recorder. In some cases, this was a General Electric recording millivoltmeter with a sensitivity of 500 millivolts for full-scale deflection and a two-speed time axis with speeds of 6 inches per minute and 6 inches per hour. This recorder has the distinct advantage of being able to record a continuous curve. Therefore, it was used almost exclusively for recording the initial elongation and the initial portion of the creep curve. The other recorder, which was installed when the creep units were moved, was a Honeywell six-point recorder with a 500-millivolt range for full-scale deflection and a chart speed of 12 inches per hour. It can record the strains from all six creep units, or all six channels can be connected to one capacitance unit in order to get the complete shape of the curve when a specimen is creeping rapidly. However, this recorder works on the basis of synchronized print, which means it will not print until the circuit is balanced. Hence, it will not record any extremely rapid movements such as take place in initial elongation.

The choice of materials to be used in the extensometer arms was limited to those materials which were resistant to oxidation at elevated temperatures and would retain rigidity at these temperatures. The capacitance plates must be conducting. While the plates could be made of aluminum, since they were outside the furnace, the extensometer arms had to be made of stainless steel. Transite or Bakelite was used to insulate the plates from the rest of the extensometer.

The units were calibrated using a micrometer-screw technique, where the micrometer screw was driven by a large wheel. The wheel had been calibrated previously and one division on the wheel was found to represent 50 microinches. The micrometer was mounted so that a rod  $1/2$  inch in diameter could be driven down and would be forced up by a spring upon reversing the direction of the micrometer. The lower half of the extensometer was mounted on the stationary rod. Then the plates were moved together until they touched. This was indicated by the shorting of the circuit, which caused the recorder to go off scale. They were opened just enough to be off of shorting, and calibration started from that point. Then the plates were opened in 0.000250-inch steps until the range over which the extensometer would be operating had been calibrated. In the sensitive portion of the curve, the calibration of each extensometer was rechecked by moving only one division, or 50 microinches, in each step. The calibration of each extensometer was checked several times and was found to repeat both in sensitivity and in zero readings.

#### Tensile-Testing Equipment

Tensile testing was carried out in a Baldwin-Southwark universal testing machine which has a 2,000- to 20,000-pound capacity and controls for various head speeds. The strains were measured by a modification of the clip-gage extensometer with standard SR-4 strain gages. The extensometer clamps onto the specimen at the upper and lower ends of the gage section. A pair of rods connected to one clamp and a pair of concentric tubes connected to the other clamp are used to transmit the movement of the specimen. Each rod is connected to the tube around it by a semi-circular clip gage, with one strain gage on the inside and one on the outside of the clip. The total output of the four strain gages is connected in series in order to detect strains as small as 50 microinches. Gimbal grips were used to hold the specimen in order to allow transverse displacement resulting from slip and to allow the slip planes to rotate toward the tension axis relatively freely with increasing strain.

## PREPARATION OF CRYSTALS

## Strain-Anneal Method of Growing Single Crystals

The strain-anneal method, which has been discussed more fully in reference 2, consists briefly of the following steps:

(1) The specimens are machined to the desired shape and size from cold-rolled bar stock. (In these experiments, a 3-inch gage length was machined to a standard 0.505-inch diameter in the center of a 6-inch length of 3/4-inch-diameter bar stock, and the ends were threaded.)

(2) The specimens are annealed for 6 hours at 550° C to produce a uniform grain size with a mean linear dimension of approximately 5 millimeters.

(3) Then the gage length of the specimens is strained permanently 1 to 1.5 percent in tension.

(4) The specimens are again placed in an annealing furnace at 450° C, and the temperature is increased 20° C per day until it reaches 635° C, at which point the specimens are left for 48 hours before cutting off the power to the furnace and allowing them to cool.

This method of growing single crystals has the very definite advantage that it produces single crystals, at least in the gage length, of specimens which are ready for creep or tensile testing without further machining. Additional machining, which would be necessary with crystals grown from the melt by the Bridgman technique, would greatly distort crystals as soft as the aluminum crystals used in this investigation. Results previously reported (ref. 2) indicate that the critical resolved shear stress of these high-purity crystals at room temperature is only 20 to 30 psi, and little more than normal handling will deform them permanently.

## Surface Preparation

The preparation of the surface of the single-crystal specimens subsequent to growth is important if any examination of the surface is to be made, after deformation has taken place, by X-ray diffraction, electron microscopy, or ordinary metallographic methods. After growth of the crystal the first step in surface preparation is to etch the surface until any grain boundaries become apparent in the gage length of the specimen, or until it becomes quite apparent that there are no grain boundaries in this region and the entire gage length is made up

of only one single crystal. The latter is not too common. However, many of the crystals have a single crystal extending over at least 2 inches of the gage length, and usually 50 to 80 percent of the specimens from a given anneal have a single crystal longer than 1 inch in the gage section, and, consequently, can be used for testing. The etch used in this investigation consisted of 50 parts hydrochloric acid, 48 parts nitric acid, and 2 parts hydrofluoric acid by volume. The fact that the cube faces of aluminum etch preferentially and become shiny gives a good indication of the orientation of the specimen before determining it accurately by back-reflection X-ray techniques.

The surfaces of these specimens can be improved, that is, made smoother, by a chemical polish consisting of 80 parts of 85 percent concentrated phosphoric acid, 15 parts of glacial acetic acid, and 5 parts of 70 percent concentrated nitric acid at a temperature of 150° to 160° F. The specimens were chemically polished in many cases when it seemed important to have a smooth surface to examine for strain markings subsequent to testing.

The smoothness of the surface, however, is not the most important consideration when preparing specimens to be studied after testing by plastic- or oxide-replica techniques with an electron microscope. The prime factor in this case is being able to prepare a specimen surface which is free of oxide. Heidenreich and Schockley (ref. 4) accomplished this by removing any oxide film just prior to tensile testing and making the replicas within 5 hours. However, aluminum oxidizes slightly even at room temperature in the times usually encountered in creep tests, and precautions must be taken to protect the prepared surface in some manner. At present work in progress utilizes an electropolished surface which has been lightly etched to produce cubic etch pits, resulting in a three-dimensional viewing of slip bands. Attempts are also being made to protect the surface at elevated temperatures and at prolonged exposure at room temperature by means of a protective coating or an atmosphere or vacuum furnace.

#### Orientation Determination

The orientation of each specimen, or the largest single crystal in the gage section that was used in this investigation, was determined by the Laue back-reflection X-ray technique. The orientations of the cube faces and the slip planes and slip directions are presented in table 1 for the three most probable slip systems. The angle between the normal to the slip plane and the specimen axis is designated as  $\phi$ . The angle between the slip direction and the specimen axis is given as  $\lambda$ . The letters A, B, C, and D identify the various (111) slip planes, and the letters U, V, W, X, Y, and Z indicate the [110] slip directions lying in these slip planes. The last three columns, headed  $\alpha$ ,  $\beta$ , and  $\psi$ , give the angles the cube faces make with the specimen axis.

Additional high-resolution X-ray work, now being pursued in conjunction with experiments designed to determine the effects of different types of prestraining on the creep phenomena, has shown the unstrained crystals to be very nearly perfect for metallic crystals although not so nearly perfect as a calcite crystal. Line breadths measured at half maximum intensity are reported to be of the order of 6 seconds of arc for a calcite crystal and about 1,500 seconds (25 minutes) of arc for an aluminum single crystal (ref. 5). The breadth of a line at half maximum intensity was about 5 to 6 minutes of arc for a typical unstrained aluminum single crystal grown by the strain-anneal method. However, this width included both the  $\alpha_1$  and  $\alpha_2$  wave lengths, since it was measured on a principal reflection in the front-reflection region, and the natural width of the reflection for 1 wave length would be even less.

#### EXPERIMENTAL PROCEDURE

Extreme care must be taken when mounting the extensometer on the single-crystal specimen to avoid damaging the crystal and, in the case of the capacitance extensometer, to make sure that the capacitance plates are parallel. Movement of nonparallel plates produces errors in the measured strains which cannot be corrected with the use of the calibration curve. As pointed out before, the low critical resolved shear stress for these pure single crystals of aluminum means they can be bent very easily, and bent or prestrained crystals yield erroneous data. After mounting the crystal in the extensometer, this whole unit is mounted in the appropriate testing unit inside a furnace. After packing asbestos around the upper and lower adapters at the open ends of the furnace, the furnace temperature is leveled off at the desired temperature.

In tensile testing the specimen was pulled as soon as the temperature leveled off at the desired value. After the first 1 percent normal strain, during which the head movement was maintained low enough to obtain data on the first portion of the stress-strain curve, the head speed was maintained constant at 0.02 inch per minute. The most important factor in these tests, or in any of the other tests involving strains greater than a few percent, was to make contact with the specimen at the correct point. Since the thickness of the specimen decreases in the direction of slip because of the rotation of the slip direction toward the specimen axis, the extensometer must be attached to the specimen at right angles to the slip direction. This can be accomplished quite easily with knowledge of the predicted slip direction from table 1.

The constant-load-rate tests were carried out in one of the creep units equipped with a lever arm with a 9:1 ratio. The creep equipment

is quite a bit lighter and easier to work with than the tensile-testing equipment. The load was measured by a spring balance inserted between the lever arm and the weight pan. This load was applied by using a vibrator to regulate the flow of shot into a bucket on the weight pan at a constant rate of 3 to 5 pounds per minute. The extension was measured with the capacitance-type extensometer connected to the photoelectric recorder.

In the creep tests the specimens were allowed to remain at temperature for a period of time, usually overnight, before applying the load in order to provide ample time for stabilizing the temperature of the specimen and the testing equipment. The load was applied directly by releasing a hydraulic jack holding the weight pan. As a matter of technique, a 50-pound weight was placed between the weight pan and the ram of the jack to insure that the ram of the jack would move away from the load and allow the full weight of the load to be applied to the specimen. Thus, the load was applied gradually, without impact. The signal from the capacitance extensometer was recorded initially by the photoelectric recorder and later by either the same recorder or the electronic recorder, depending on the number of tests in progress.

## EXPERIMENTAL RESULTS

### Stress-Strain Curve From Tensile Tests

In conjunction with this extensive program on creep of the single crystals of aluminum, it appeared profitable to supplement this work with the determination of the stress-strain curve for the single crystals of aluminum of the particular purity that was used, namely, 99.99+ percent. This line of reasoning was prompted by some prior results from tensile tests at very low strains which indicated that the critical resolved shear stress at room temperature increased by an order of magnitude when the purity of the aluminum was decreased from 99.99+ to 99.95 percent (ref. 2). The purposes of these tests were manifold. The effect of temperature on the stress-strain curve could be compared with the effect of temperature on the creep curve. Specimens which had been deformed rapidly could be compared with the creep specimens with respect to strain markings. The resulting stress-strain curves yielded some idea of the strains to be expected from various stresses on the aluminum single crystals, especially with regard to initial elongation in creep tests. The resulting curves can be compared with other stress-strain curves reported in the literature, in particular, those by Boas and Schmid in reference 3 for aluminum single crystals of lower purity.

The data (stress  $\sigma$  against extension  $\epsilon$ ) from the tensile tests were converted to shear stress  $\tau$  and shear strain  $\gamma$  in order to

correct for the rotation of the crystal lattice with extension. The lattice rotates in such a manner as to decrease the angle between the slip direction and the specimen axis. The manner in which the shear stress varies during extension is given by the following equation (ref. 6):

$$\tau = \sigma \cos \phi \left(1 - \frac{\sin^2 \lambda}{d^2}\right)^{1/2} \quad (1)$$

where  $\phi$  and  $\lambda$  are the angles defined in the section "Orientation Determination" and  $d = (1 + \epsilon) = l/l_0$ , or the ratio of the instantaneous length to the initial length. For values of the extension less than 1 percent, the resolved shear stress is given with about 1 percent inaccuracy by the equation

$$\tau = \sigma \cos \phi \cos \lambda \quad (2)$$

The resolved shear strain is affected also by the lattice rotation. It should be remembered that the shear strain is not simply the extension resolved along the slip plane, but it is the relative displacement of two slip planes a unit distance apart. The shear strain (plastic only) has also been described analytically by Schmid and Boas (ref. 7) in terms of the original orientation and extension by the relation

$$\gamma = \frac{1}{\cos \phi} \left[ (d^2 - \sin^2 \lambda)^{1/2} - \cos \lambda \right] \quad (3)$$

For strains of 1 percent or less, this relation is given with 1 percent inaccuracy by

$$\gamma = \epsilon / \cos \phi \cos \lambda \quad (4)$$

Tensile tests to at least 15-percent extension were carried out in the same temperature range, 82° F to 400° F, in which the creep tests were run. A family of curves pointing out the effect of temperature on the stress-strain curve is shown in figure 5. The stress required to produce a given strain decreased with increasing temperature, as expected, except in cases where the orientation of the crystals was such as to induce duplex slip early in the plastic deformation. However, some difficulty was experienced in duplicating a stress-strain curve at a given temperature. In some cases there was considerable difference in the shapes of the curve, especially in the early portion. Two such specimens,

the curves for which are plotted in figure 6, exhibited what appeared to be a certain amount of nonhomogeneous yielding in the early portion of the curve, followed by an approximately linear stress-strain curve. Although the inhomogeneity occurred in the beginning of the test, when the strain rate was not constant, it is interesting to note that both these specimens had slip directions which made angles greater than  $45^\circ$  with the specimen axis. This might be responsible for the easy yielding in the first part of the curve, because the glide is enhanced as the slip direction rotates toward  $45^\circ$ . The strain-hardening in all specimens appeared to vary over the range of strains investigated.

Some other discrepancies were found which could not be attributed to differences in orientation or the proximity of any of the orientations to duplex slip. The only reasonable explanation appeared to be that some of these crystals were strained prior to testing while being mounted in the heavy tensile-testing equipment. To check this point, it was decided to determine the stress-strain curve utilizing the lighter equipment used in the creep tests.

#### Stress-Strain Curve From Constant-Load-Rate Tests

The family of curves obtained in constant-load-rate tests at various temperatures is shown in figure 7. Good reproducibility was obtained in repeating the stress-strain curve at a given temperature, except when the crystal orientation was oriented preferably for duplex slip or the early onset of duplex slip. In general, the curves in figure 7 have the same shape and stress level as those from tensile tests in figure 5, although plotted on different scales. Although the curves from these tests cannot be superimposed exactly on those from the tensile tests, still, the stress required to produce a given strain decreased with increasing temperature with the exception of those crystals in which duplex slip was observed.

The effect of duplex slip on the stress-strain curve is shown in figure 8. The control curves from figure 7 are dashed in for comparison, and the highest and second highest values of  $\cos \phi \cos \lambda$ , the factor which determines the slip direction with the highest resolved shear stress, are tabulated in figure 8. Crystal P-164, which started out in duplex slip, was very much harder to strain than crystal P-163 at the same test temperature,  $200^\circ \text{ F}$ . Crystal P-152 at  $400^\circ \text{ F}$  and crystal P-162 at  $300^\circ \text{ F}$  did not start out in duplex slip but were oriented favorably for it after some rotation of the initial glide planes.

### Creep Curve

The creep data obtained in this investigation were in the temperature range from room temperature (82° F) to 400° F at resolved-shear-stress levels of 200, 300, and 400 psi. The range of stresses used in this temperature range was limited on the low side by the stress required to produce measurable creep and on the high side by the desire to maintain the constant-load tests as approximately constant stress tests.

Typical curves of shear strain against time for the crystals are shown in figures 9 and 10. The extensions have been converted to shear strains by the simple relation (equation (4)):

$$\gamma = \epsilon / \cos \phi \cos \lambda$$

The curves appear to have a continually decreasing slope, or creep rate. Whether an approximately constant slope is observed or not depends largely on the time scale chosen. This point is illustrated graphically in figures 9 and 10, where the total shear strain has been plotted against time scales in both seconds and hours. Both curves tend toward approximately constant slopes in both time plots. However, the magnitudes of the slopes from the two time scales differ considerably, with the slope from the second scale being approximately the initial slope of the curve on the hour scale.

In an attempt to determine an empirical relation for the creep curve, the data were plotted in logarithmic coordinates. A typical case is that of crystal P-165, for which data are plotted in figure 9 in rectangular coordinates. The logarithmic plot of total shear strain against time for this crystal yields a curve which is concave upward. If the measured initial shear strain is subtracted before plotting the data, the logarithmic plot yields a curve which is concave downward. A straight line is obtained on logarithmic coordinates over an extended range of strains only when a shear strain somewhat smaller than the experimentally measured initial shear strain is subtracted from the total shear strain. The justification for this modification of the experimental data is that the measured initial shear strain contains some time-dependent strain. Experimental data confirming the above ideas on the nature of the creep curve also have been obtained by Hazlett, Parker, and Hansen in an independent investigation (ref. 8). However, it was felt that the more desirable approach was to determine the creep rates from the slope of the strain-time curve, rather than adjusting the experimental data to produce a straight line on a logarithmic plot which then could be described analytically.

Because of the high sensitivity of the measuring equipment, the major portion of this investigation has been directed toward creep in the low strain region, particularly the so-called transient or early portion of the creep curve. In order to remain in the region of approximately constant stress, even at the highest stresses and temperatures investigated, and to pick a time interval in which reliable data could be obtained from all creep tests, it was decided to analyze the curves for creep rates over the first  $2\frac{1}{2}$  hours, even though the data for some of the tests appeared to be reliable out to 100 hours. A typical working curve from which to determine creep rates is plotted in figure 11.

Some difficulty was experienced in determining the creep rate from some of these curves of shear strain against time at short times (1 to 10 minutes) because of the occurrence of an S-shaped strain-time curve in some instances, as depicted in figure 12 for crystal P-115 tested at 200° F and 300-psi resolved shear stress. This type of curve had been observed previously by Cottrell and Aytakin (ref. 6) with zinc single crystals but at somewhat higher strains. These authors attributed this type of curve to inhomogeneous deformation resulting from the first deformed region's acting in such a manner that the rotation of the lattice accompanying glide more than compensated for the work-hardening. This would cause the deformed region to act as if it were softer and, hence, confine the deformation to those regions which had deformed first. They observed this type of curve for specimens, with high values of the angles between the slip direction and the specimen axis and between the slip plane and the specimen axis, which were creep-tested at slow strain rates at elevated temperatures above 120° C. The occurrence of the S-shaped curves in this investigation could not be explained as resulting from a specific orientation of the specimen axis with respect to the principal crystallographic directions (a standard projection). Neither could this occurrence be correlated with a certain type of initial orientation of the active slip system, which is determined by the angles the slip direction and the normal to the slip plane make with the specimen axis. Such curves could be attributed only to the internal state of the crystal and to the fact that this may have been altered by small amounts of pre-straining which occurred during the handling and mounting of the specimens for testing. The S-shaped curves were predominant at low stresses, as would be expected on this basis.

The only radical effect of orientation on the creep curve that was observed was the effect of having two slip systems oriented equally favorably. Figure 13 illustrates the effect of duplex slip on the creep curve at 200° F with 200-psi resolved shear stress, and figure 14, the same effect for crystals tested at 300° F with 400-psi resolved shear stress. In both cases the initial strain and the slope of the curve have been reduced substantially.

### Strain Markings

The round shape of the specimens is both advantageous and disadvantageous for observing strain markings resulting from plastic deformation. The round shape enables observations to be made at any angular position around the specimen axis. However, the curvature of the surface makes it exceedingly difficult to obtain photographs of the specimens with the whole field in focus, especially at the higher magnifications. Characteristic of the aluminum crystals, in particular, is the oxide film which covers the surface after an elevated-temperature test in air, and even after prolonged exposure to air at room temperature. This oxide film, which also hindered photographing the strain markings on the specimens, appeared to form less rapidly on the chemically polished surface than on an etched surface.

Although slip bands, which apparently consisted of one or more slip lines, appeared straight to the eye, they turned out to be somewhat wavy at a magnification of 400X. Pictures were taken through an eyepiece with a calibrated scale in which one division was equivalent to 22 microns in order to show approximate slip-band spacings and slip-band widths. At low strains, in the range of 1 to 2 percent, the deformation was not uniform over the gage length of the specimen. Also, it was more difficult to distinguish between scratches and strain markings at low strains. Typical photographs of the strained regions on some creep specimens are shown in figure 15. These photographs were taken approximately perpendicular to the specimen axis and approximately parallel to the  $\theta$ -direction of the slip plane in order to standardize the portion of the slip bands photographed as that part at the end of the major axis of the ellipse in which the slip bands intersect the specimen surface. From these optical micrographs, although the structure of the slip bands cannot be determined, it is possible to state that the width of the slip bands increases with the temperature at which the specimens have been deformed for a given resolved shear stress. If a wider slip band corresponds to more slip per band, or more individual slip lines per band, then it can be concluded that, for a given amount of strain at a given resolved shear stress, a higher temperature results in a lower slip-band density. The nonconformity of the deformation at the lower strains and stresses makes it difficult to extend this argument further to state definitely the dependence of the observed slip-band density on the resolved shear stress or the strain while holding all other variables fixed. However, if the width of each slip band or the amount of slip in each band is determined largely by the temperature during deformation, then one intuitively would expect the slip-band density to increase with increasing strain or time while holding the temperature and stress constant. The fact that the observed slip bands invariably have turned out to be ellipses which outlined the predicted slip plane is good evidence that slip is one of the mechanisms of creep, and probably the predominant one.

Observations were also made on the specimens extended in a tensile test or in a constant-load-rate test to at least 15-percent elongation. Figure 16(a) was obtained in a manner similar to that used in photographing the creep specimens, while figure 16(b) was taken perpendicular to the specimen axis and also perpendicular to the  $\theta$ -direction of the slip plane, instead of parallel to it. These two pictures point out two important facts: The deformation is quite uniform over the entire specimen which has been extended 18 percent; and, from figure 16(b), it can be seen that the slip bands appear to be much thinner near the minor axis of the ellipse which the slip bands make in intersecting the specimen surface. The latter figure shows why the position at which the slip bands were observed must be standardized and also why the extensometers must be attached to the specimens in such a manner as to make contact perpendicular to the  $\theta$ -direction of the slip direction.

With regard to the terminology of strain markings, the term "slip band" has been reserved for the sharp markings which were observed on the specimens under a microscope at a magnification of 400X. Although a slip band may consist of only a single slip line, the structure of the slip band with respect to the number of individual slip lines in it must be determined with an electron microscope in detailed studies, such as those of Heidenreich and Schockley (ref. 4) and of Brown (ref. 9). Besides the slip bands, other markings were found on the tensile specimens and the creep specimens experiencing more than 2- or 3-percent extension. These markings, which are shown in figure 16(c), had two distinct properties. They intersected the sharper slip bands at approximately right angles, and they were broad enough to disappear under a magnification of 100X to 400X, resembling a "rumpling" of the surface. These markings have been described recently and referred to as "deformation bands" by Chen and Mathewson (ref. 10). The fact that these markings are perpendicular to the slip bands is in agreement with Chen and Mathewson, who asserted that the slip direction is the pole of the deformation bands. These same markings have been referred to also as "kink bands" by Honeycombe (ref. 11), Cahn (ref. 12), Calnan (in a discussion of ref. 10), and Pratt (ref. 13).

For orientations near poles, crystal P-166, with its axis near the [100] direction, exhibited definite kink bands (see fig. 16(c)), but crystal P-152, with its axis near the [110] direction, did not produce distinct kink bands.

Figure 16(d) illustrates a portion of a specimen outside of the gage length used in tensile testing this specimen at 203° F. This part, containing a grain boundary, shows the strength of a grain boundary at 203° F with respect to resistance to the propagation of slip across the boundary and the occurrence of slip in two different directions in the bicrystal.

## ANALYSIS OF RESULTS

## Stress-Strain Curve

A family of stress-strain curves has been obtained for single crystals of aluminum at various temperatures. However, these curves are in considerable disagreement with the curves previously published by Boas and Schmid (ref. 3) and by Taylor and Elam (ref. 14). While Taylor and Elam's work was restricted primarily to room-temperature tests, the work of Boas and Schmid was performed in the temperature range from  $-185^{\circ}\text{C}$  to  $600^{\circ}\text{C}$ . Furthermore, they used round specimens very similar to those used in this investigation. The only apparent discrepancy between their work and the work reported here is in the purity of the aluminum used. However, this factor, the purity of the single crystals, appears to be sufficient to explain this discrepancy.

The increase in purity from 99.63 percent used by Boas and Schmid to 99.99+ percent used in this investigation was enough to reduce the resolved shear stress required to reach a given shear strain by almost half (see fig. 5). Since prior results of this investigation already have shown that an increase in purity from 99.95 to 99.99+ percent was sufficient to decrease the critical resolved shear stress by an order of magnitude, it seems quite reasonable that the difference in purity of the specimens would account for the rather large discrepancy between the stress-strain curves reported here and those reported by Boas and Schmid. These results give strong evidence of the propagation of slip by means of the movement of dislocations, in view of the manner in which impurity atoms are thought to tie down dislocations and retard the propagation of slip. Cottrell has treated rather extensively the effect of solute atoms on the behavior of dislocations (ref. 15).

The analysis of the stress-strain curves can be carried still further by application of some of the ideas and relationships proposed by Taylor (ref. 16) and extended and discussed by Koehler (ref. 17). Koehler modified Taylor's work to obtain the following expression for the resolved shear stress:

$$\tau = 2\pi G \left( \frac{2\lambda}{L} \right)^{1/2} \left( \frac{2\pi m}{m-1} \right) \gamma^{1/2} \quad (5)$$

In this equation,  $G$  is the shear modulus,  $\lambda$  is the distance between nearest neighbors,  $m$  is the reciprocal of Poisson's ratio, and  $L$  is an internal dimension, assumed to be of the order of the mosaic block. Typical values (taken from ref. 17) for aluminum single crystals are:  $G$  equals  $2.655 \times 10^{11}$  dynes per square centimeter,  $\lambda$  equals

$2.855 \times 10^{-8}$  centimeter, and Poisson's ratio equals 0.343. However, equation (5) was obtained only after setting up a simple physical picture and relationship for the distance between dislocations of like sign in terms of the amount of plastic strain that has taken place. Also, the assumption was made that the distance between dislocations of like sign is equal to the distance  $a$  between dislocations of opposite sign to obtain the relation:

$$a = (\lambda L / 2\gamma)^{1/2} \quad (6)$$

Koehler's analysis of the room-temperature stress-strain curve reported by Taylor and Elam (ref. 14), which agreed quite well with the stress-strain curve at room temperature reported by Boas and Schmid, yielded the value of  $2.8 \times 10^{-4}$  centimeter for the characteristic distance  $L$  and a value of  $2 \times 10^{-6}$  centimeter for  $a$ , the distance between dislocations at a resolved shear strain of 1.2.

A similar analysis of the stress-strain curve from crystal P-106 (see fig. 5) yielded the considerably larger value of  $7.6 \times 10^{-4}$  centimeter for  $L$  and the value of  $7.4 \times 10^{-6}$  centimeter for the spacing between dislocations at a resolved shear strain of 0.2. Increasing the shear strain to 1.2 would only decrease this spacing to  $4.3 \times 10^{-6}$  centimeter. With due regard for their limited accuracy, the above numbers have been presented primarily for comparison of the work reported here with that of other workers in the field. The implication of Koehler's analysis above is that there are fewer boundaries, such as mosaic boundaries, to impede the propagation of slip by means of movement of dislocations in these high-purity crystals of aluminum than there were in the single crystals of previous workers. The parabolic relation between shear strain and shear stress arises on theoretical grounds from the postulation of a square array of positive and negative dislocations equally spaced.

#### Creep Curve

Mott and Nabarro (ref. 18), in their treatment of transient creep, developed a relation based on the movement of dislocation loops. The chance  $\alpha$  per unit time that a loop of a dislocation will move is given by

$$\alpha = v e^{-[G(\sigma)/kT]} \quad (7)$$

where  $\nu$  is the frequency of vibration of a dislocation in its potential trough,  $G(\sigma)$  is the activation energy for movement of a dislocation loop,  $k$  is Boltzmann's constant, and  $T$  is the absolute temperature. Assuming that a dislocation which has moved enters an unfavorable region and cannot move again, then the number of dislocations in the stress range from  $\sigma$  to  $\sigma + d\sigma$  will diminish according to the relation

$$N(\sigma, t) = N(\sigma, 0)e^{-\alpha t} \quad (8)$$

For reasonable values of  $\alpha$  and  $t$ ,  $N(\sigma)$  is essentially constant and hardening takes place by the exhaustion of the available dislocations. On this basis, these authors arrive at an expression for the creep strain, namely,

$$\epsilon_c = \text{Constant } T^{2/3}(\log_e \nu t)^{2/3} \quad (9)$$

where  $\nu$  is of the order of  $10^8$ . This expression should be valid only as long as  $N(\sigma)$  is approximately constant. This condition implies that the stress and temperature are low enough that the generation of new dislocations is negligible. Also, the condition has been imposed that the creep strain cannot exceed the initial elongation upon loading. This result is characteristic of the "exhaustion" hypothesis.

For most cases of interest in this investigation, the creep strain did exceed the initial elongation, so this analysis cannot apply. However, even at the low stresses in room-temperature tests, when the condition that  $N(\sigma)$  be essentially constant might be fulfilled, the condition is not fulfilled that is obtained by differentiating equation (9), namely,

$$t\dot{\epsilon} = \text{Constant}(\log_e \nu + \log_e t)^{-1/3} \quad (10)$$

Therefore, Mott and Nabarro's theory requires that the product  $t\dot{\epsilon}$  decrease with time, and in such a manner that a plot of  $(t\dot{\epsilon})^{-3}$  against the logarithm of time is a straight line increasing with time. This was not found to be the case, even in the low-stress tests at room temperature.

Another theory of transient creep has been proposed by Smith (ref. 19). He assumes that, at the instant when the initial (instantaneous) extension is complete, there exist in the specimen a very large number of stress-concentration spots where the local stress is higher than the mean applied stress but lower than the local yield stress. This

will occur where dislocations become trapped at energy barriers such as impurity atoms and crystallite or mosaic boundaries. Each of these spots of stress concentration can be characterized by an activation energy  $E$  such that a local stress fluctuation, caused by thermal agitation, will raise the stress in a volume  $V$  to the yield stress and initiate glide at that point. The significance of the volume  $V$  is that the stress fluctuation must occur in a large enough volume for the local glide process not to be annihilated by the elastic forces in the surrounding region after the stress fluctuation has closed.

This theory possesses essentially the same shortcoming as Mott and Nabarro's theory. Although the variation with time of the distribution function  $f$  of the number of spots characterized by activation energies between  $E$  and  $E + dE$  can be postulated, the initial distribution immediately after initial extension is not known. Assuming the initial distribution of spots to be constant, Smith arrives at a relation for the creep strain, namely,

$$\epsilon_c = AT \log_e(\beta t) \quad (11)$$

where  $A$  and  $\beta$  are constants. The creep rate is given by the expression:

$$\dot{\epsilon} = AT(1/t) \quad (12)$$

Although the time dependence predicted by this theory is reasonable, the temperature dependence is much too weak, as is the case in Mott and Nabarro's theory with respect to this latter point.

A third mathematical description of transient creep, one derived on an empirical basis, was proposed by Andrade (ref. 20) and later applied to single crystals by Cottrell and Aytakin (ref. 21). Neglecting the viscous component of creep, the expression for the shear strain is

$$\gamma = \gamma_0 + \beta t^{1/3} \quad (13)$$

where  $\beta$  and  $\gamma_0$  are constants, and  $\gamma_0$  is the instantaneous shear strain upon loading. Differentiating equation (13), one obtains the expression for the shear strain rate

$$\dot{\gamma} = \frac{1}{3} \beta t^{-2/3} \quad (14)$$

The creep data have been analyzed in terms of shear strain rates in order to eliminate the ambiguity in determining the initial shear strain, which seemed to differ in two crystals tested under the same experimental conditions. The results are presented in figures 17(a) to 17(c) for the 200-, 300-, and 400-psi resolved-shear-stress tests, respectively, at various temperatures in the range from room temperature to 400° F. As can be seen from these plots of the logarithm of the shear strain rate against the logarithm of the time, the results agree quite well with the time dependence predicted by the Andrade relation, especially at the two higher stresses, up to times of about 2 hours. This is in agreement with the relation between strain rate and time for polycrystals, thus providing a link between the behavior of single-crystal and polycrystalline materials. These curves, although not always linear, appear to tail off at the longer times. This change is opposite to that which would be expected either on the basis of an increase in stress due to a reduction in cross section or rotation of the glide planes or on the basis of the onset of secondary creep, in which case the creep rate would tend toward a constant value instead of decreasing with time.

At present the stress and temperature dependences of the shear strain rate appear to be more complex. From these data the stress dependence has been investigated and found to follow a power law ( $\dot{\gamma} \propto \tau^n$ ) approximately. The power  $n$  varied from about 4 to 5, with no apparent or systematic variation at the different temperatures.

Because of the scatter in the data, the exact form of the temperature dependence could not be determined. Attempts were made to fit the data empirically to functions of the form  $e^{T/T_0}$ ,  $e^{-Q/RT}$ , and  $T^m$ , where  $T_0$ ,  $Q$ , and  $m$  are constants and  $R$  is the universal gas constant. Plotting the logarithm of shear strain rate at a given time and stress against absolute temperature gave families of straight lines with less scatter than was found with any of the other methods of analyzing the data. The activation-energy relation ( $\dot{\gamma} \propto e^{-Q/RT}$ ) did not predict so high a strain rate at the higher temperature as was observed. However, this may just be a reflection of some inaccuracy in the determination of the shear strain rate at room temperature. The data also were fitted to a  $T^m$  relation, with significant scatter in the plots and with  $m$  varying slightly with temperature but being of the order of 10 or slightly higher. Therefore, additional experiments, which are now in progress, at higher temperatures and different stresses will be necessary to determine the exact form of the temperature and stress dependences of the creep rate or shear strain rate and the appropriate constants.

## DISCUSSION OF PLASTIC DEFORMATION IN LIGHT OF PRESENT IDEAS ON DISLOCATION THEORY

In addition to the recent work on specific problems, such as the work on aluminum which has already been mentioned, a very comprehensive survey of the information on plastic deformation of solids was written by Seitz and Read in 1941 (ref. 22). Much of the recent work has been an attempt to explain the plastic properties of solids by means of dislocation theory, as evidenced by the reports of various conferences (refs. 23 and 24).

The need for the postulation of crystalline imperfections such as mosaics and dislocations arose when the experimentally determined critical resolved shear stress (the stress necessary to produce plastic deformation) was found to be lower by a factor of about 1,000 than the theoretical shear strength for a perfect crystal. Theoretical calculations indicated that Hooke's law should hold for much higher shear stresses, up to about  $G/2\pi$ , where  $G$  is the shear modulus (ref. 25).

Dislocations enhance plastic flow in the early stages by permitting plastic deformation to take place more easily than would be possible in an ideally perfect crystal. However, they are also responsible for strain-hardening in the later stages of plastic deformation. This results from the interaction of the dislocations and their associated stress fields. This interaction increases and tends to resist further deformation as more and more dislocations are produced in deforming a solid. Thus, the dislocation theory has been successful in explaining almost any of the physical situations occurring in plastic deformation, at least in a qualitative manner. Examples of this are thermal hardening and strain-softening, pointed out by Orowan (ref. 25). The evidence for thermal hardening was the fact that zinc crystals which were strained plastically and then given a rest of 24 to 48 hours at room temperature (at which zinc crystals show comparatively rapid thermal softening) required stresses considerably above the previously applied stress before plastic deformation would take place. The evidence for strain-softening was the manner in which a soft steel wire is bent. The soft steel wire bends in the shape of a polygon, indicating that the strained regions soften and, hence, deformation is confined to limited regions. This is in contrast with a copper wire, which can be bent into a circular loop, indicating that deformation is not confined to deformed regions.

In recent years considerable work has been reported on the generation, motion, and annihilation of dislocations in which the qualitative theories are being extended gradually to obtain quantitative results as the knowledge of plastic deformation increases (refs. 22 to 27). These treatments

have indicated that, when exhaustion creep, such as that proposed by Mott and Nabarro, fails, the ideas of Seitz, that transient creep is related to the movement of available dislocations and secondary or steady-state creep is related to the rate of generation of dislocations, appear to be more appropriate to describe creep phenomena. Frank and Read have contributed greatly to this field with their ideas on the generation of dislocations by a multiplication process for slow-moving dislocations (ref. 28). A geometrical configuration of the lattice of the type proposed by Frank and Read which leads to the production of vacancies under applied stress has been termed a generator. Cessation of these generators apparently takes place after about 1,000 dislocation rings have been produced. The simplest explanation of the cessation of the generator appears to be that it is destroyed systematically after it has formed this number of rings. The simplest objection to this idea seems to be that it does not give an obvious explanation of the hardening of latent slip planes, unless it is assumed that the debris left by the generator when it vanishes is effective in inhibiting further generation which would produce slip in latent planes. Moreover, it does not explain the observation that metals may be resoftened to their original high ductility by annealing, as if the generation could be reconstituted easily. This suggests the possibility that the generator is not destroyed but only jammed by a process which prevents it from forming new dislocations without producing any geometrical change.

The yield point in some metallic crystals has been explained on the basis that mosaic-block boundaries act as dislocation traps. Plastic deformation does not take place until the dislocations are given enough energy by means of external stress or thermal energy to surmount the barriers presented by the mosaic boundaries. After this happens, considerable glide takes place before strain-hardening sets in. Cottrell has discussed the yield point in single-crystal and polycrystalline metals with respect to the release of anchored dislocations in the presence of internal stresses and the effect of neighboring dislocations on the stress required to free a dislocation (ref. 29).

Taylor first interpreted work-hardening on the basis of dislocation theory (ref. 16) and pointed out that dislocations exert forces on one another. He stated that dislocations of like sign repel one another and dislocations of unlike sign attract one another. Thus, as the deformation of an initially unstrained crystal proceeds, large numbers of dislocations become trapped in the interior of the crystal. The forces acting between dislocations do not allow one dislocation to pass freely by another one. A larger and larger stress is necessary to strain the crystal by moving dislocations through it as the material becomes work-hardened.

Besides the effect of impurity atoms on the critical resolved shear stress and the stress-strain curve, other evidence enhances the status

of dislocation theory in explaining plastic deformation. The first such evidence is the manner in which the initial elongation or initial shear strain varied in the creep tests. The initial shear strain was determined largely by the shear stress; that is, its dependence on the stress was very strong, while the dependence on temperature was considerably weaker. This type of dependence is what one would expect on the basis that increasing the stress would free a larger number of dislocations, those released between the stresses  $\sigma$  and  $\sigma + d\sigma$ , whereas an increase in the temperature would increase only the number of dislocations activated by energy from thermal fluctuations. The second evidence is the manner in which duplex slip has affected the creep curves and the stress-strain curves. Although this can be explained on a macroscopic scale by work-hardening, work-hardening itself has been explained in terms of dislocation theory. This leads to the thought that the reduction of initial elongation and subsequent creep rate, and the increase in the stress-strain curve due to duplex slip, results from the interaction of the dislocations and their associated stress fields when they try to propagate strains by means of slip through regions which already have been strained.

### CONCLUSIONS

An investigation of the creep of single crystals of aluminum at temperatures from room temperature to 400° F indicated the following conclusions:

1. The shear strain rate of the aluminum single crystals follows Andrade's relation approximately over a time interval up to about 2 hours. The agreement is better for the higher stresses.
2. The slope of the strain-time curve appears to decrease continuously with increasing time, and the existence of an approximately constant slope depends only upon the magnitude of the time scale chosen.
3. The effect of duplex slip is to reduce considerably the initial elongation and the slope (or creep rate) of the creep curve. The slope of the stress-strain curve is increased (i.e., a higher stress is required to obtain a given strain) by the onset of duplex slip.
4. The observation of the strain markings on the crystals indicated that slip played an important role in the deformation both by creep and by straining in tension with an increasing load.
5. The stress-strain curve for these high-purity aluminum single crystals is considerably lower than that reported for aluminum single crystals of less purity. This result is in agreement with the fact that the critical resolved shear stress increases with decreasing purity, which

was determined earlier in this investigation, and with the idea that solute atoms tend to tie down the available dislocations and retard plastic deformation.

6. Analysis of the stress-strain curve and X-ray examination of these high-purity aluminum single crystals have indicated that the crystals are very nearly perfect for metallic crystals.

7. The results presented in this report can be described adequately in a qualitative manner by the present state of the theory of dislocations.

Battelle Memorial Institute,  
Columbus, Ohio, July 10, 1952.

## REFERENCES

1. Schwofe, A. D., and Jackson, L. R.: A Survey of Creep in Metals. NACA TN 2516, 1951.
2. Schwofe, A. D., Shober, F. R., and Jackson, L. R.: Creep in Metals. NACA TN 2618, 1952.
3. Boas, W., and Schmid, E.: Über die Temperaturabhängigkeit der Kristallplastizität. Zs. Phys., Bd. 71, 1931, pp. 703-714.
4. Heidenreich, R. D., and Schockley, W.: Study of Slip in Aluminum Crystals by Electron Microscope and Electron Diffraction Methods. Conf. on Strength of Solids, Phys. Soc. (London), 1948, pp. 57-75.
5. Barrett, Charles S.: Structure of Metals. First ed., McGraw-Hill Book Co., Inc., 1943, pp. 220-221.
6. Cottrell, A. H., and Aytakin, V.: The Flow of Zinc Under Constant Stress. The Jour. Inst. Metals, vol. 77, 1950, pp. 389-423.
7. Schmid, E., and Boas, W.: Plasticity of Crystals With Special Reference to Metals. F. A. Hughes and Co., Ltd. (London), 1950.
8. Hazlett, T. H., Parker, E. R., and Hansen, R. D.: The Nature of the Creep Curve. Rep. No. CAO-55, Ninth Tech. Rep., Ser. No. 28, Issue No. 14, Inst. Eng. Res., Univ. of Calif., Jan. 1952.
9. Brown, A. F.: Fine Structure of Slip Zones in Aluminum. Nature, vol. 163, no. 4155, June 18, 1949, pp. 961-962.
10. Chen, N. K., and Mathewson, C. H.: Structural Studies of Plastic Deformation in Aluminum Single Crystals. Jour. Metals, vol. 3, no. 8, Aug. 1951, pp. 653-660. (See also Discussion by E. A. Calnan, Jour. Metals, vol. 4, no. 5, May 1952, pp. 526-527.)
11. Honeycombe, R. W. K.: Inhomogeneities in the Plastic Deformation of Metal Crystals. The Jour. Inst. Metals, vol. 80, pt. 2, Oct. 1951, pp. 45-56.
12. Cahn, R. W.: Slip and Polygonization in Aluminum. The Jour. Inst. Metals, vol. 79, pt. 3, May 1951, pp. 129-158.
13. Pratt, P. L.: Strain-Hardening of Single Crystals. AERE-M/R-883, British Atomic Energy Res. Establishment, Mar. 1952.

14. Taylor, G. I., and Elam, C. F.: The Plastic Extension and Fracture of Aluminum Crystals. Proc. Roy. Soc. (London), ser. A., vol. 108, no. 745, May 1, 1925, pp. 28-51.
15. Cottrell, A. H.: Effect of Solute Atoms on the Behavior of Dislocations. Conf. on Strength of Solids, Phys. Soc. (London), 1948, pp. 30-38.
16. Taylor, G. I.: The Mechanism of Plastic Deformation of Crystals. Proc. Roy. Soc. (London), ser. A, vol. 145, no. 855, July 2, 1934, pp. 362-404.
17. Koehler, J. S.: On Dislocation Theory and the Physical Changes Produced by Plastic Deformation. Am. Jour. Phys., vol. 10, no. 6, Dec. 1942, pp. 275-285.
18. Mott, N. F., and Nabarro, F. R. N.: Dislocation Theory and Transient Creep. Conf. on Strength of Solids, Phys. Soc. (London), 1948, pp. 1-19.
19. Smith, C. L.: A Theory of Transient Creep in Metals. Proc. Phys. Soc. (London), vol. 61, pt. 3, no. 345, Sept. 1, 1948, pp. 201-205.
20. Andrade, E. N. daC.: On the Viscous Flow in Metals and Allied Phenomena. Proc. Roy. Soc. (London), ser. A, vol. 84, no. 567, June 9, 1911, pp. 1-12.
21. Cottrell, A. H., and Aytakin, V.: Andrade's Creep Law and the Flow of Zinc Crystals. Nature, vol. 160, no. 4062, Sept. 6, 1947, pp. 328-329.
22. Seitz, F., and Read, T. A.: The Theory of the Plastic Properties of Solids. Parts I-IV. Jour. Appl. Phys., vol. 12, no. 2, Feb. 1941, pp. 100-118; vol. 12, no. 3, Mar. 1941, pp. 170-186; vol. 12, no. 6, June 1941, pp. 470-486; vol. 12, no. 7, July 1941, pp. 538-554.
23. Anon.: Conference on Strength of Solids. Phys. Soc. (London), 1948.
24. Anon.: Symposium on the Plastic Deformation of Crystalline Solids. Carnegie Inst. Tech. and Office of Naval Res., NAVEXOS-P-834, May 19-20, 1950.
25. Orowan, E.: Problems of Plastic Gliding. Proc. Phys. Soc. (London), vol. 52, pt. 1, no. 289, Jan. 1, 1940, pp. 8-22.
26. Burgers, J. M.: Geometrical Considerations Concerning the Structural Irregularities to be Assumed in a Crystal. Proc. Phys. Soc. (London), vol. 52, pt. 1, no. 289, Jan. 1, 1940, pp. 22-23.

27. Seitz, F.: On the Generation of Vacancies by Moving Dislocations. *Advances in Phys.*, vol. 1, no. 1, Jan. 1952, pp. 43-90.
28. Frank, F. C., and Read, W. T., Jr.: Multiplication Processes for Slow-Moving Dislocations. *Symposium on the Plastic Deformation of Crystalline Solids*, Carnegie Inst. Tech. and Office of Naval Res., NAVEXOS-P-834, May 19-20, 1950, pp. 44-49.
29. Cottrell, A. H.: The Yield Point in Single Crystal and Polycrystalline Metals. *Symposium on the Plastic Deformation of Crystalline Solids*, Carnegie Inst. Tech. and Office of Naval Res., NAVEXOS-P-834, May 19-20, 1950, pp. 60-76.

TABLE 1.- CRYSTALLOGRAPHIC DATA FOR ALUMINUM SINGLE CRYSTALS

Specimen	Slip plane	$\phi$ , deg	Slip direction	$\lambda$ , deg	$\cos \phi \cos \lambda$	$\alpha$ , deg	$\beta$ , deg	$\psi$ , deg
Aluminum creep specimens								
P-37	D	$\phi$ 60.0	XAD	31.0	0.429	$\alpha$ 22.0	57.5	22.5
	C	$\phi$ 61.5	ZAC	$\phi$ 29.5	.415			
	B	$\phi$ 22.0	UBC	$\phi$ 70.5	.310			
P-66	B	55.0	YAB	$\phi$ 37.5	0.455	$\alpha$ 54.5	$\phi$ 29.3	18.0
	C	$\phi$ 68.0	VAC	23.0	.345			
	D	$\phi$ 21.5	UCD	69.0	.333			
P-89	C	$\phi$ 45.0	VCD	46.0	0.491	$\alpha$ 8.0	$\phi$ 58.0	30.0
	A	30.0	ZAB	60.0	.433			
	C	$\phi$ 45.0	UBC	63.0	.321			
P-107	B	65.6	YAB	38.0	0.3255	$\alpha$ 37.3	29.5	38.0
	B	65.6	VBD	38.0	.3255			
	D	$\phi$ 73.0	WAD	30.0	.253			
P-115	C	$\phi$ 54.3	VCD	42.0	0.4337	$\alpha$ 36.6	$\phi$ 19.0	57.0
	C	$\phi$ 54.3	UBC	42.3	.3806			
	A	17.0	YAB	$\phi$ 73.0	.2796			
P-122	A	61.5	ZAB	$\phi$ 36.4	0.384	$\alpha$ 33.8	$\phi$ 44.9	25.9
	A	61.5	YAD	$\phi$ 45.3	.335			
	D	$\phi$ 70.5	VBD	26.8	.298			
P-123	C	$\phi$ 55.1	VCD	66.7	0.462	$\alpha$ 17.4	26.6	57.0
	B	66.7	XBD	$\phi$ 24.2	.361			
	A	23.0	YAB	$\phi$ 67.9	.346			
P-124	D	$\phi$ 49.6	VAD	46.8	0.444	$\alpha$ 39.7	$\phi$ 14.0	46.6
	D	$\phi$ 49.6	UCD	51.4	.404			
	B	22.1	YBC	$\phi$ 69.9	.319			
P-127	A	42.7	ZAB	$\phi$ 53.2	0.440	$\alpha$ 46.0	43.0	7.0
	A	42.7	YAD	$\phi$ 55.2	.419			
	C	28.1	WCD	65.3	.369			
P-135	A	54.0	YAD	$\phi$ 41.5	0.440	$\alpha$ 49.3	$\phi$ 34.7	18.0
	A	54.0	ZAB	$\phi$ 51.5	.366			
	C	$\phi$ 18.6	UBC	71.5	.301			
P-148	D	$\phi$ 55.2	VAD	38.9	0.444	$\alpha$ 19.2	32.7	50.5
	D	$\phi$ 55.2	UCD	52.0	.352			
	B	18.3	YBC	$\phi$ 71.8	.296			
P-150	A	51.8	YAD	$\phi$ 42.2	0.458	$\alpha$ 50.9	$\phi$ 34.3	15.8
	A	51.8	ZAB	$\phi$ 53.7	.366			
	C	$\phi$ 21.0	UBC	69.3	.330			
P-151	D	$\phi$ 58.2	VAD	42.9	0.386	$\alpha$ 22.3	40.2	41.0
	D	$\phi$ 58.2	UCD	43.2	.384			
	C	77.3	YAC	$\phi$ 22.4	.204			
P-157	C	$\phi$ 55.9	VCD	35.0	0.459	$\alpha$ 17.6	24.3	59.1
	B	64.9	XBD	$\phi$ 25.7	.382			
	A	24.4	YAB	$\phi$ 67.0	.356			
P-165	B	58.5	VBD	36.7	0.419	$\alpha$ 48.8	22.4	31.9
	B	58.5	ZAB	$\phi$ 50.2	.335			
	A	69.2	WAD	24.9	.322			

<sup>a</sup>Measured from left end of specimen. All other angles were measured from right.

TABLE 1.- CRYSTALLOGRAPHIC DATA FOR ALUMINUM SINGLE CRYSTALS - Concluded

Specimen	Slip plane	$\phi$ , deg	Slip direction	$\lambda$ , deg	$\cos \phi \cos \lambda$	$\alpha$ , deg	$\beta$ , deg	$\psi$ , deg
Aluminum tensile specimens								
P-106	A	46.0	YAB	<sup>a</sup> 48.0	0.465	20.0	<sup>a</sup> 38.0	50.0
	A	46.0	VAC	56.0	.388			
	D	<sup>a</sup> 25.5	WCD	<sup>a</sup> 65.5	.374			
P-119	C	<sup>a</sup> 45.9	VCD	45.4	0.488	<sup>a</sup> 9.3	34.1	55.4
	A	27.0	YAB	<sup>a</sup> 63.0	.405			
	C	<sup>a</sup> 45.9	UBC	59.2	.356			
P-121	D	<sup>a</sup> 54.5	VAD	40.9	0.439	<sup>a</sup> 18.9	35.6	48.0
	D	<sup>a</sup> 54.5	UCD	50.0	.374			
	B	17.5	YBC	<sup>a</sup> 72.6	.285			
P-137	A	42.7	YAB	<sup>a</sup> 49.8	0.474	<sup>a</sup> 36.3	<sup>a</sup> 52.5	6.8
	C	<sup>a</sup> 29.5	WCD	61.9	.410			
	A	42.7	XAD	<sup>a</sup> 60.0	.368			
P-138	D	<sup>a</sup> 44.5	VAD	49.6	0.462	<sup>a</sup> 9.0	38.4	49.9
	D	<sup>a</sup> 44.5	UCD	56.7	.391			
	B	26.7	ZBC	<sup>a</sup> 64.7	.381			
P-161	C	<sup>a</sup> 50.4	VCD	41.7	0.476	<sup>a</sup> 13.4	30.8	55.5
	A	24.9	YAB	<sup>a</sup> 65.3	.379			
	C	<sup>a</sup> 50.4	UBC	58.4	.334			
Aluminum constant-load-rate specimens								
P-144	D	<sup>a</sup> 49.4	VAD	44.1	0.467	<sup>a</sup> 13.3	34.8	51.8
	D	<sup>a</sup> 49.4	UCD	55.5	.368			
	B	23.4	ZBC	<sup>a</sup> 66.9	.360			
P-152	D	<sup>a</sup> 40.1	UCD	55.5	0.433	<sup>a</sup> 4.6	45.7	43.8
	D	<sup>a</sup> 40.1	VAD	57.3	.413			
	B	30.8	XAB	<sup>a</sup> 63.8	.380			
P-162	D	<sup>a</sup> 48.7	VCD	<sup>a</sup> 70.1	0.440	<sup>a</sup> 13.4	45.2	41.5
	D	<sup>a</sup> 48.7	WAD	50.9	.416			
	B	21.8	XAB	<sup>a</sup> 70.1	.316			
P-163	B	45.5	YAB	<sup>a</sup> 44.7	0.498	<sup>a</sup> 61.1	<sup>a</sup> 27.5	7.4
	D	<sup>a</sup> 32.0	UCD	58.0	.449			
	C	<sup>a</sup> 71.9	VAC	18.7	.295			
P-164	A	64.8	XAB	<sup>a</sup> 30.6	0.367	<sup>a</sup> 28.2	<sup>a</sup> 47.4	28.5
	D	<sup>a</sup> 64.7	UBD	30.9	.366			
	D	<sup>a</sup> 64.7	WAD	<sup>a</sup> 47.9	.286			
P-166	C	<sup>a</sup> 52.8	VCD	38.8	0.471	<sup>a</sup> 8.0	12.9	74.7
	A	40.2	YAB	<sup>a</sup> 54.2	.447			
	A	40.2	ZAC	<sup>a</sup> 58.4	.400			

<sup>a</sup>Measured from left end of specimen. All other angles were measured from right.

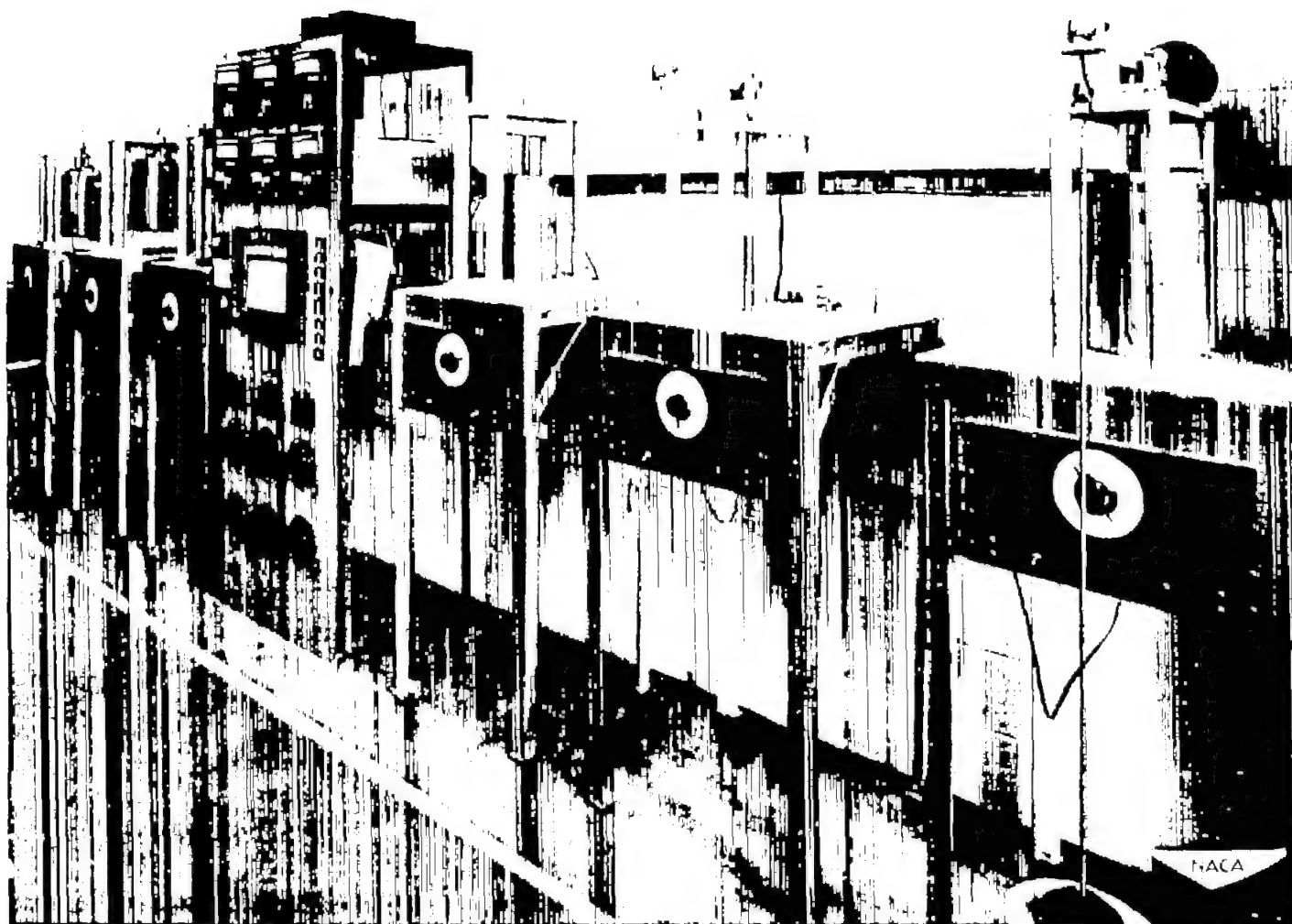


Figure 1.- Creep-testing units and control equipment.

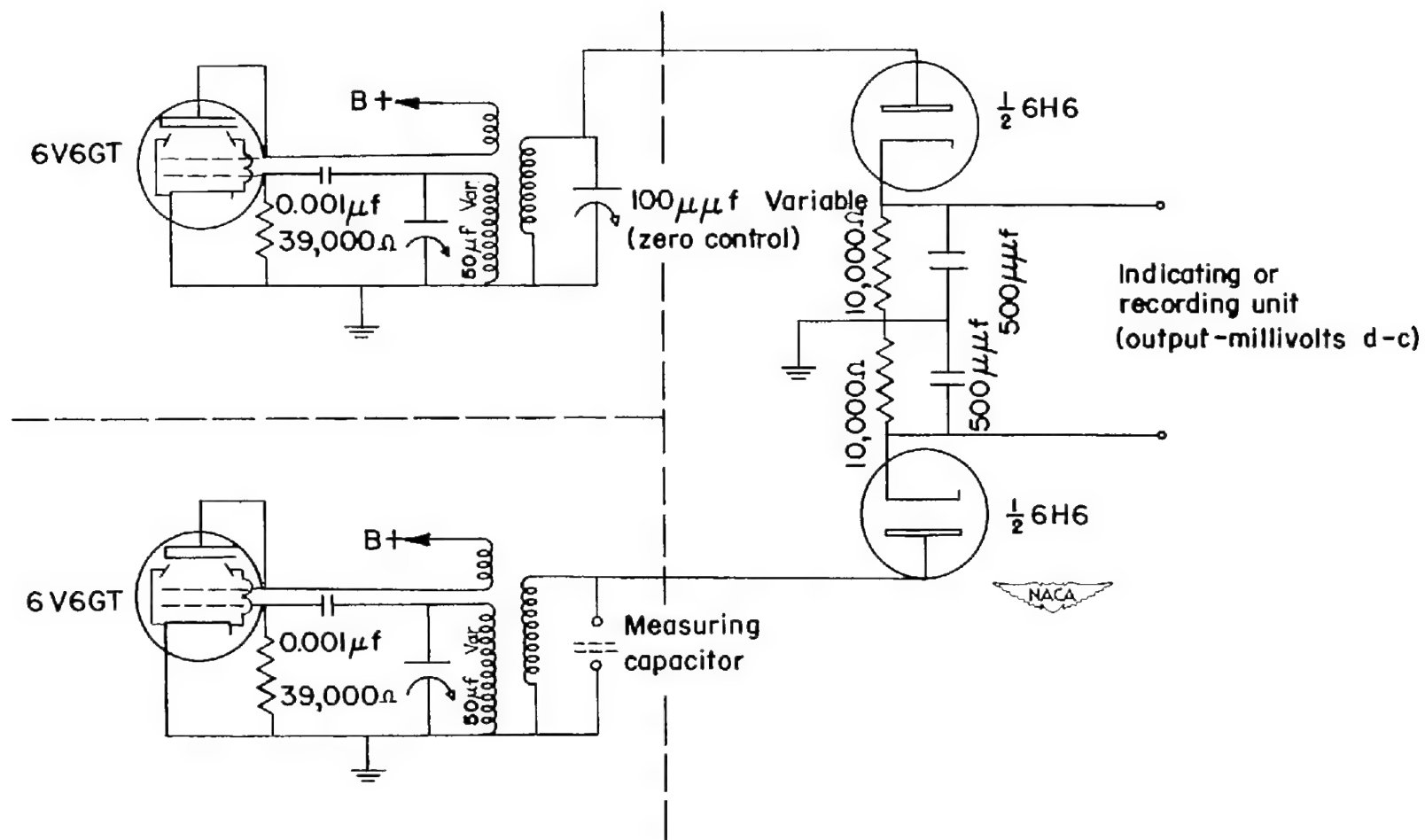


Figure 2.- Capacitance-strain-gage unit.

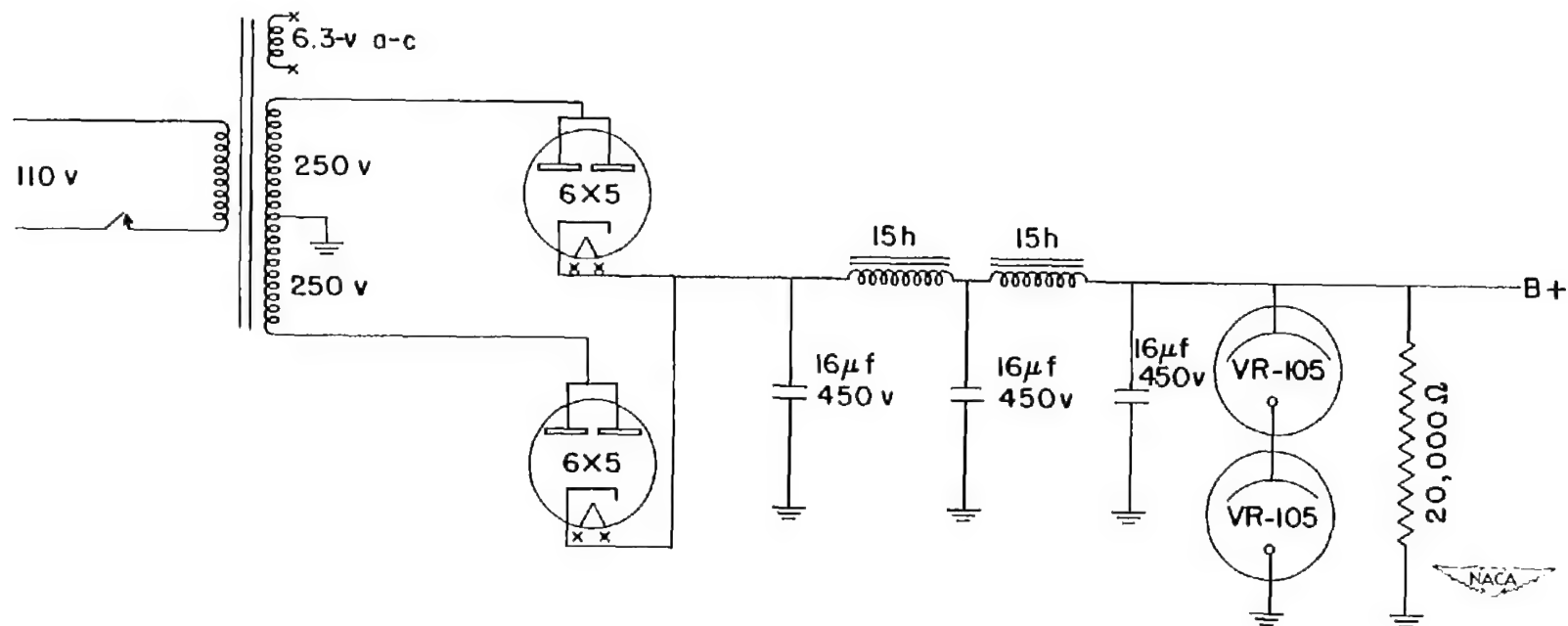


Figure 3.- Power supply.

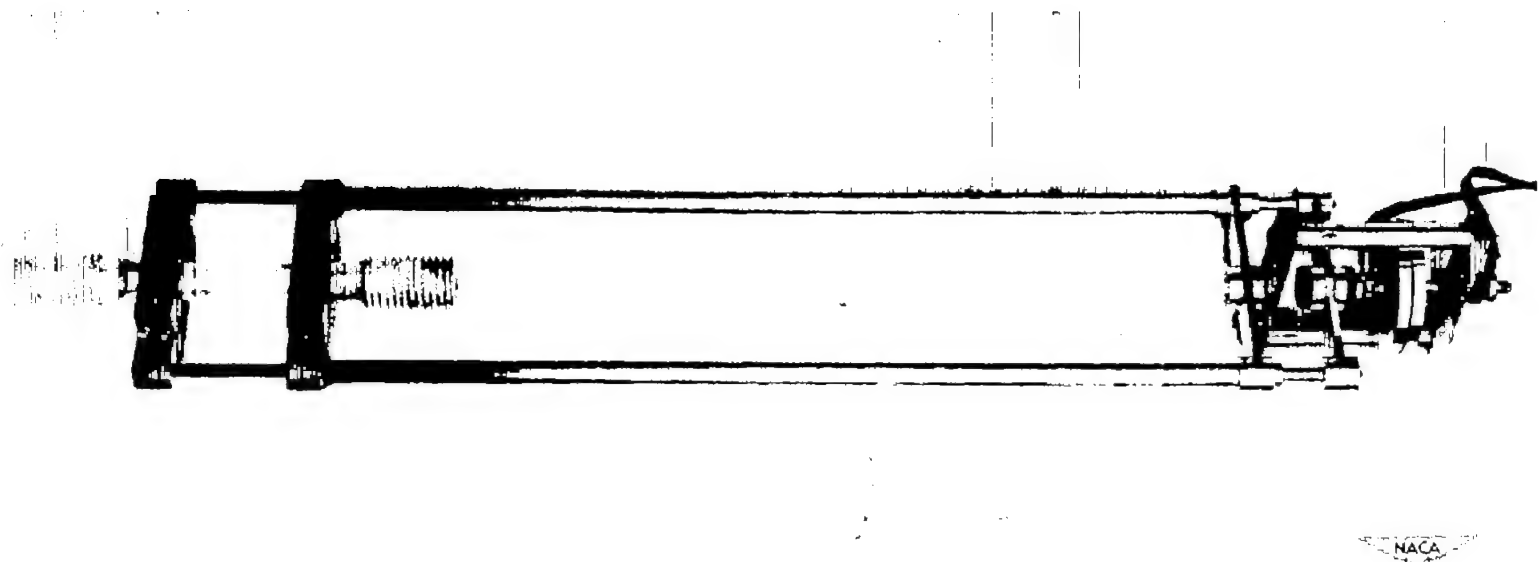


Figure 4.- Capacitance extensometer attached to a specimen.

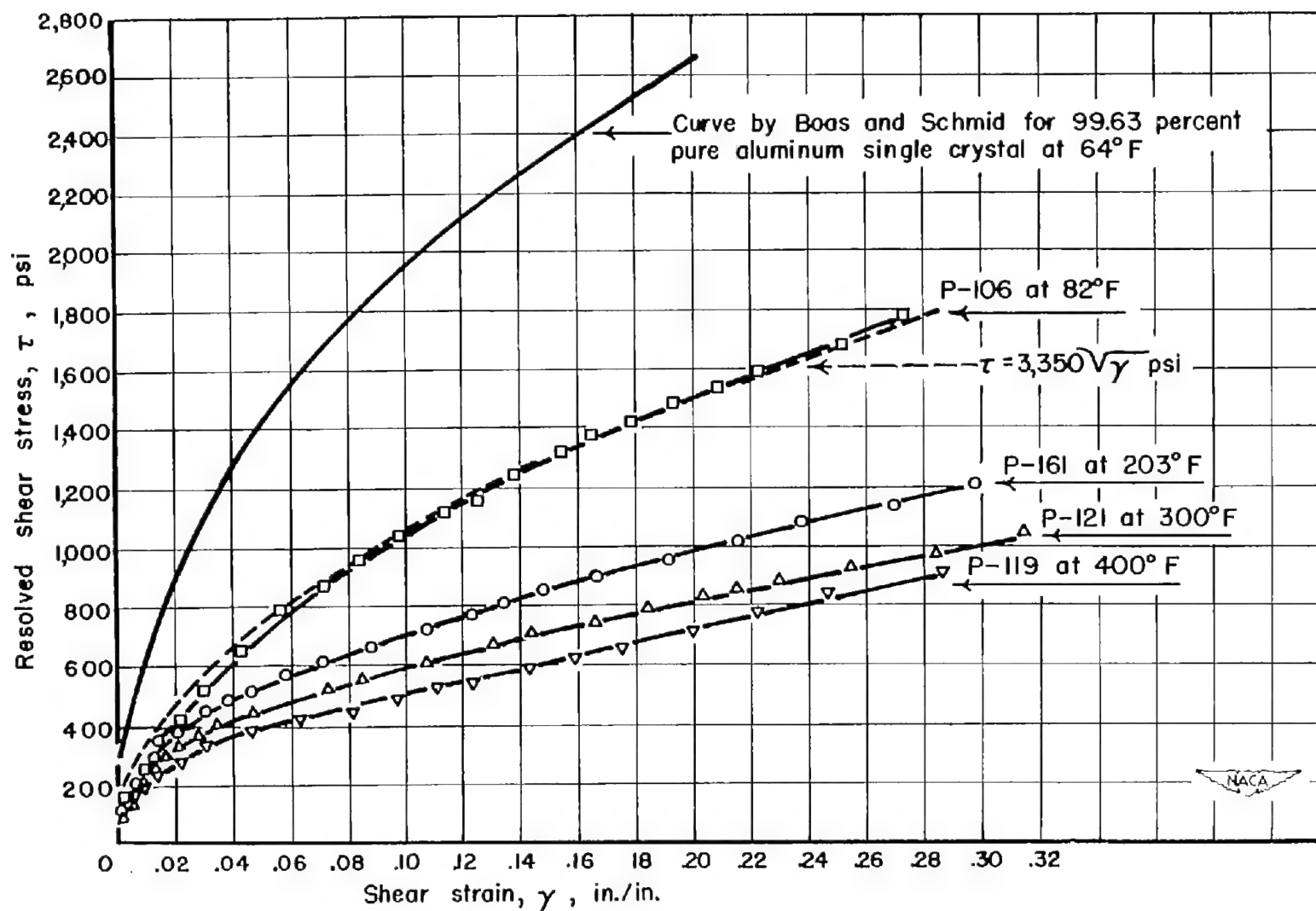


Figure 5.- Effect of temperature on tensile stress-strain curve for single crystals of aluminum.

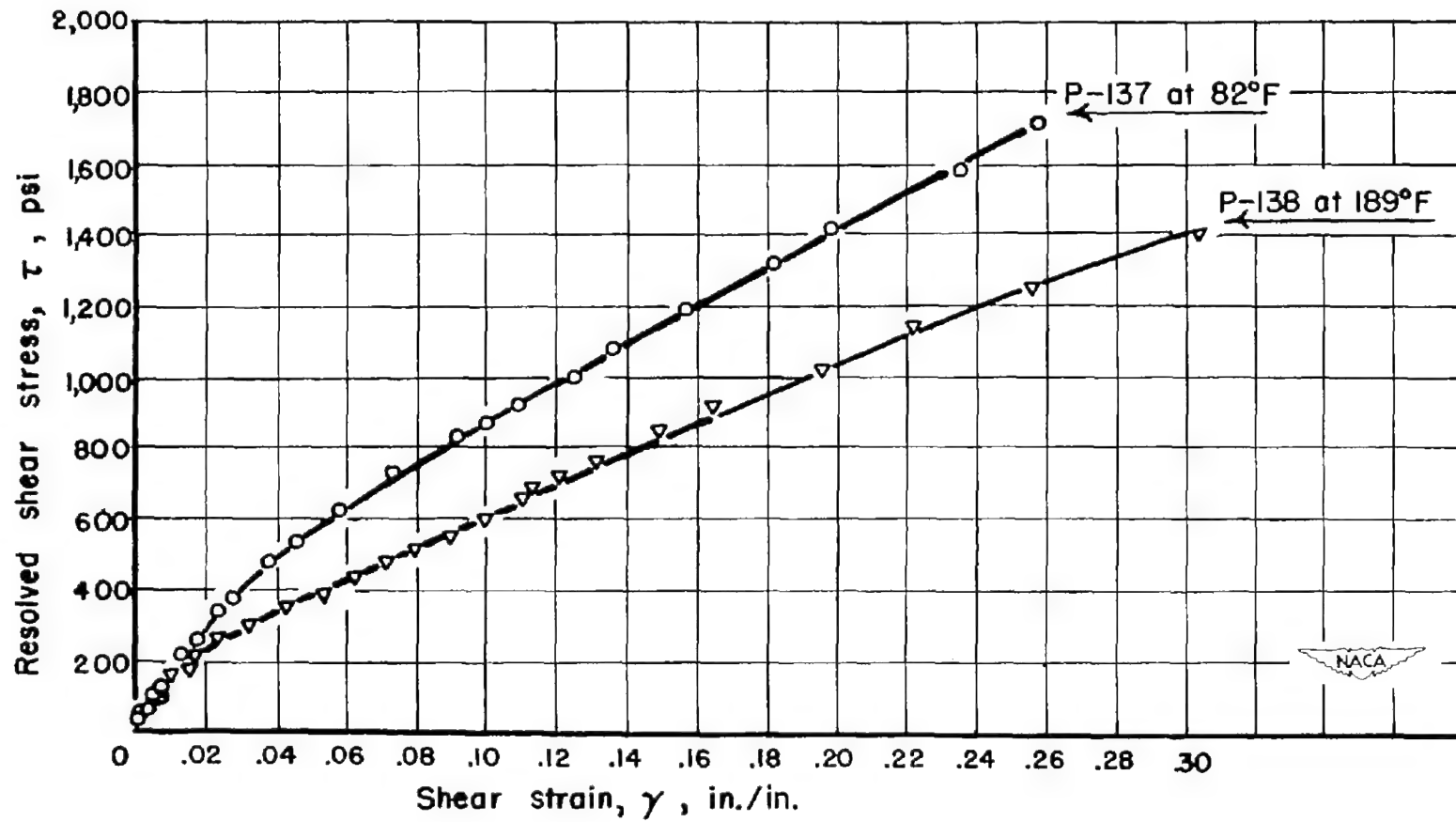


Figure 6.- Stress-strain curves from tensile tests on single crystals of aluminum with angle  $\lambda$  greater than  $45^\circ$ .

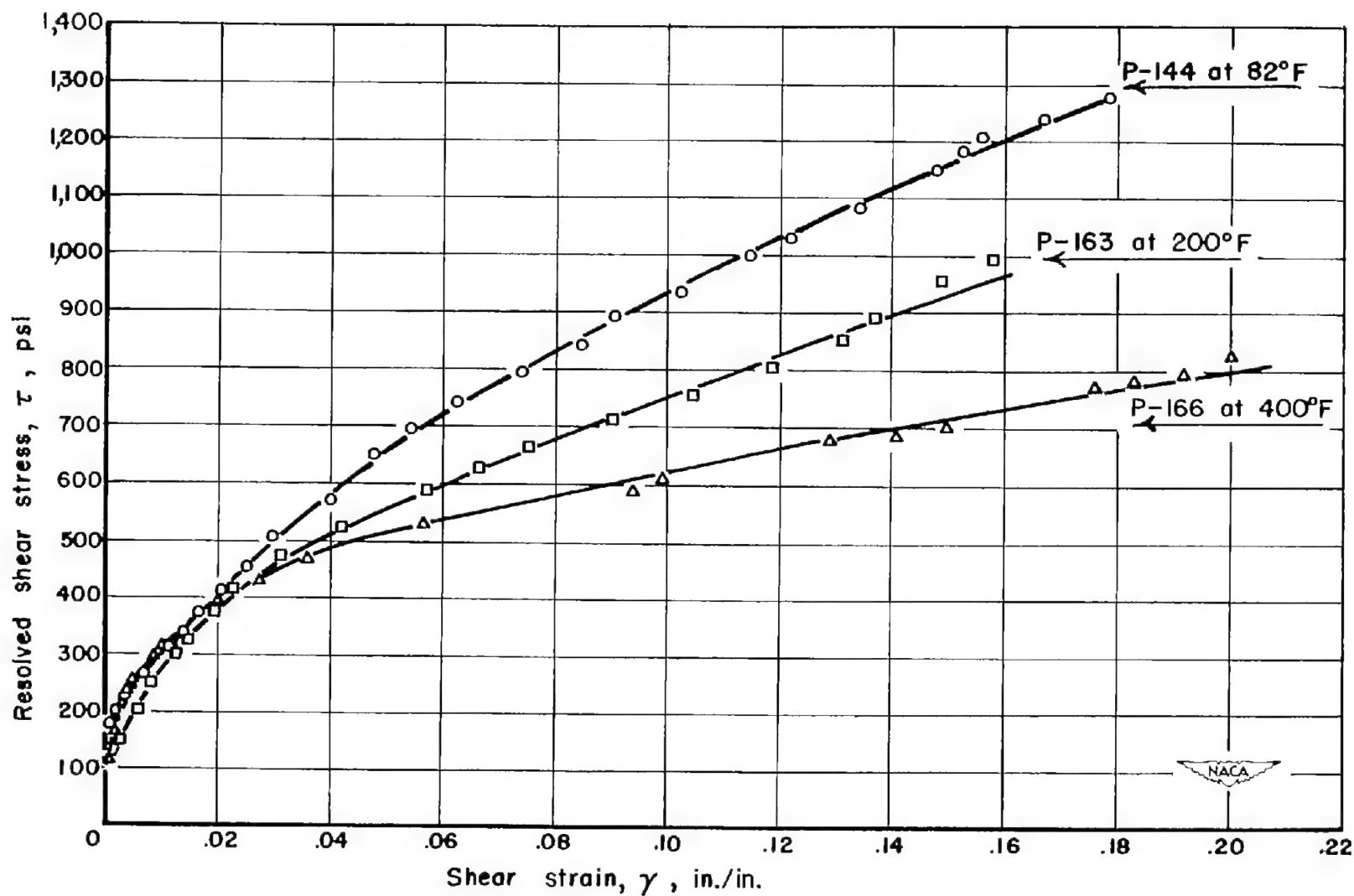


Figure 7.- Effect of temperature on aluminum-single-crystal stress-strain curves obtained in constant-load-rate tests.

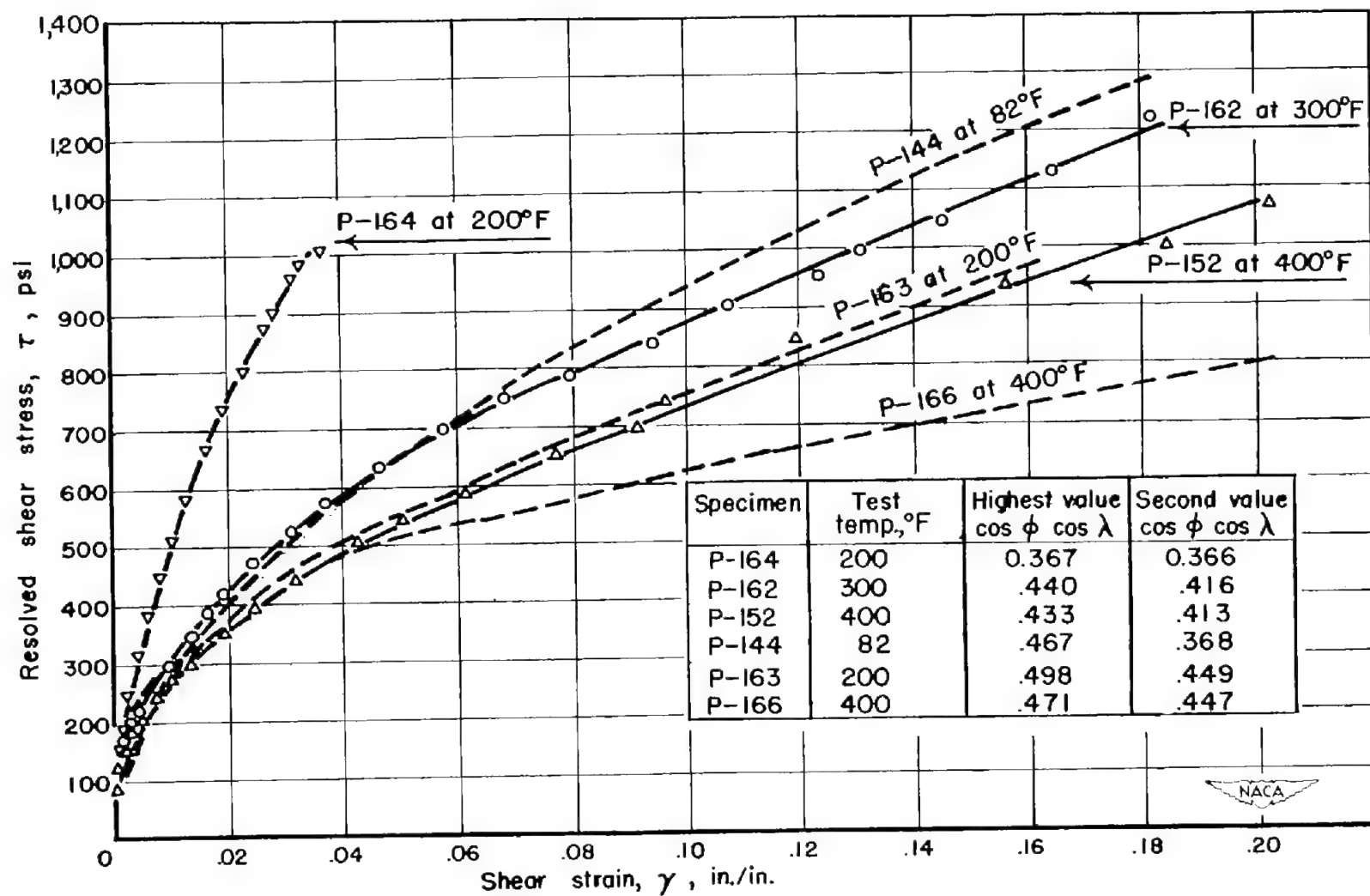


Figure 8.- Effect of duplex slip on aluminum-single-crystal stress-strain curves obtained in constant-load-rate tests.

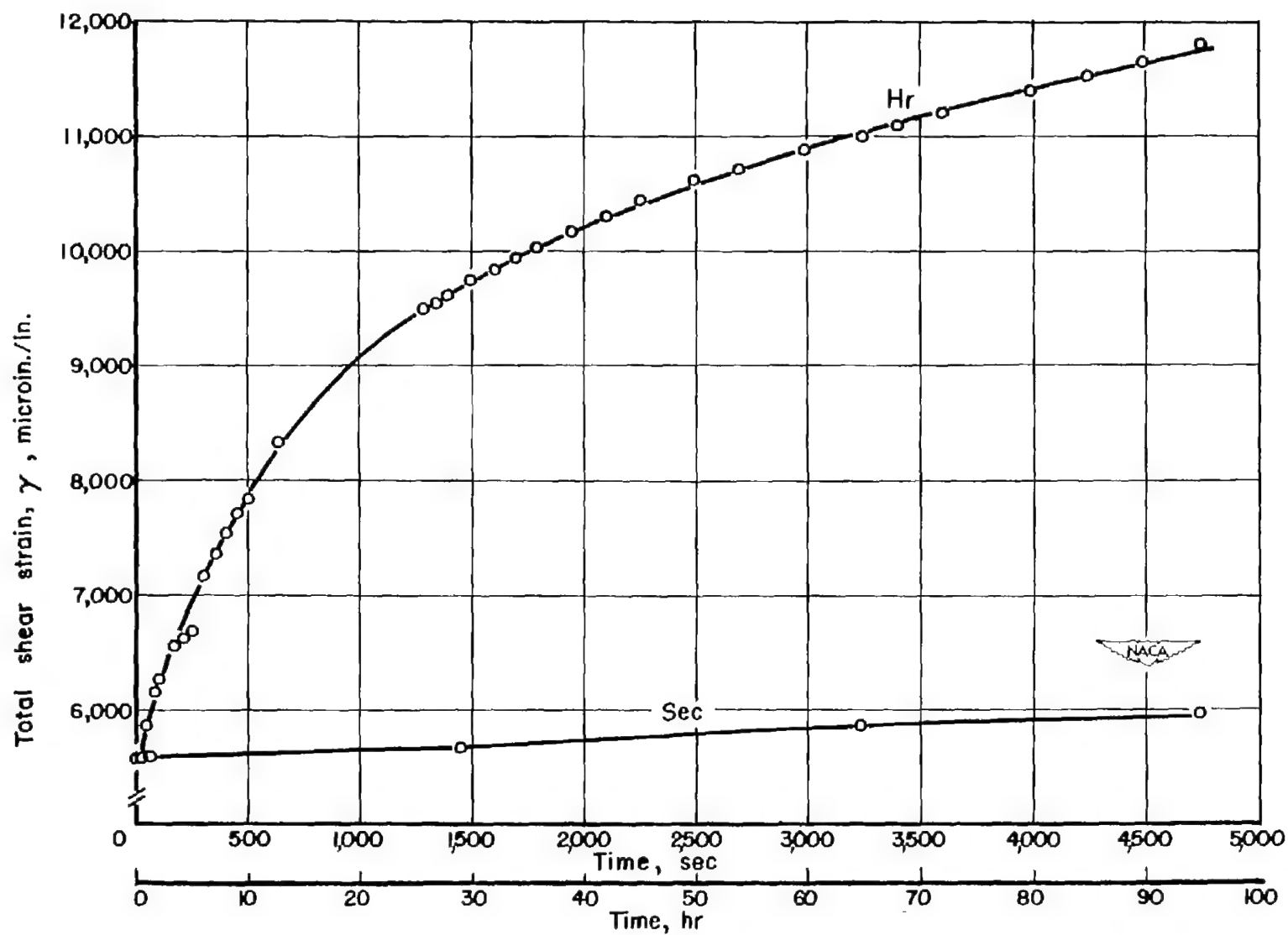


Figure 9.- Strain-time curve for crystal P-165 at 300° F with  $\tau = 200$  psi.

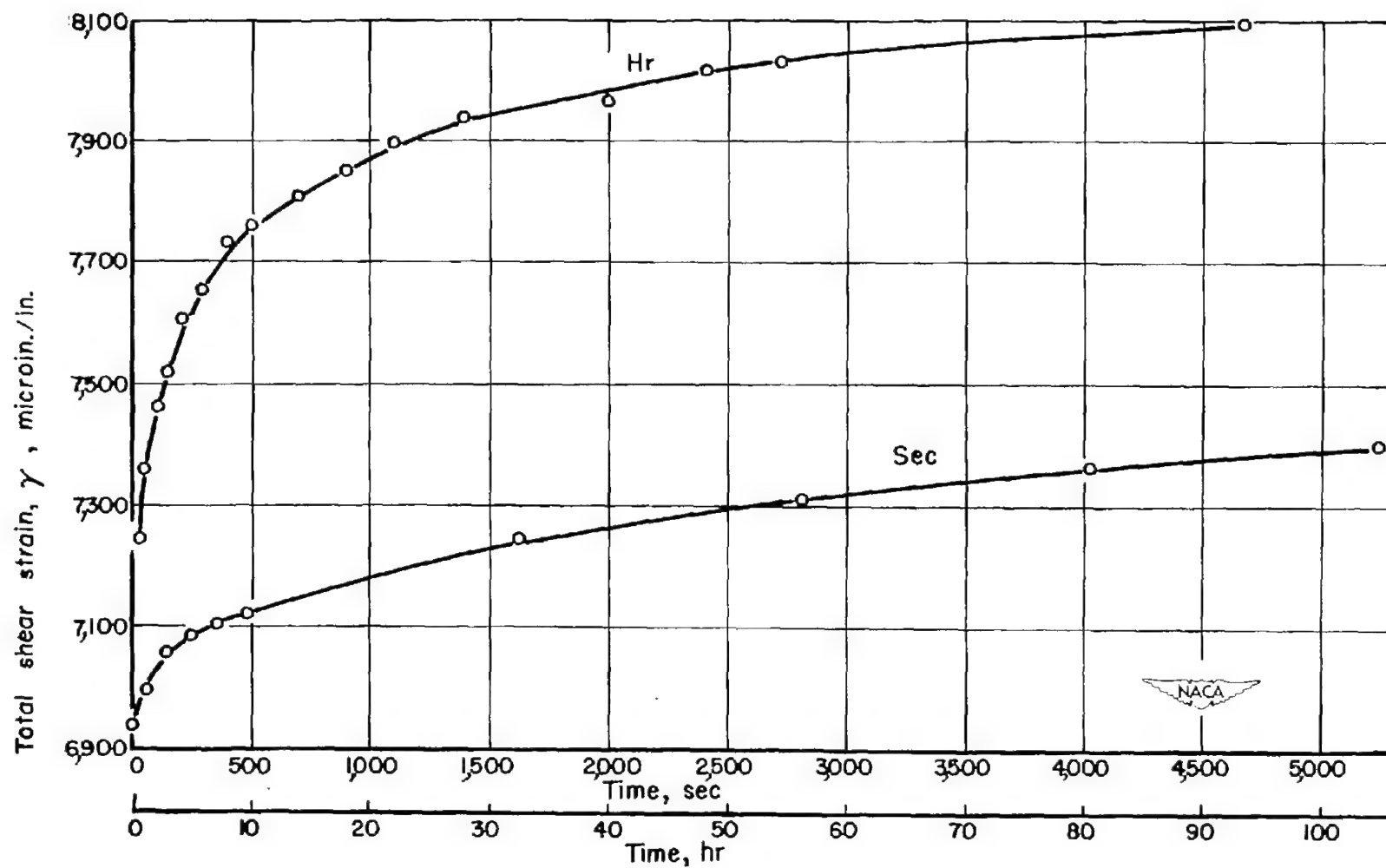


Figure 10.- Strain-time curve for crystal P-89 at 82° F with  $\tau = 300$  psi.

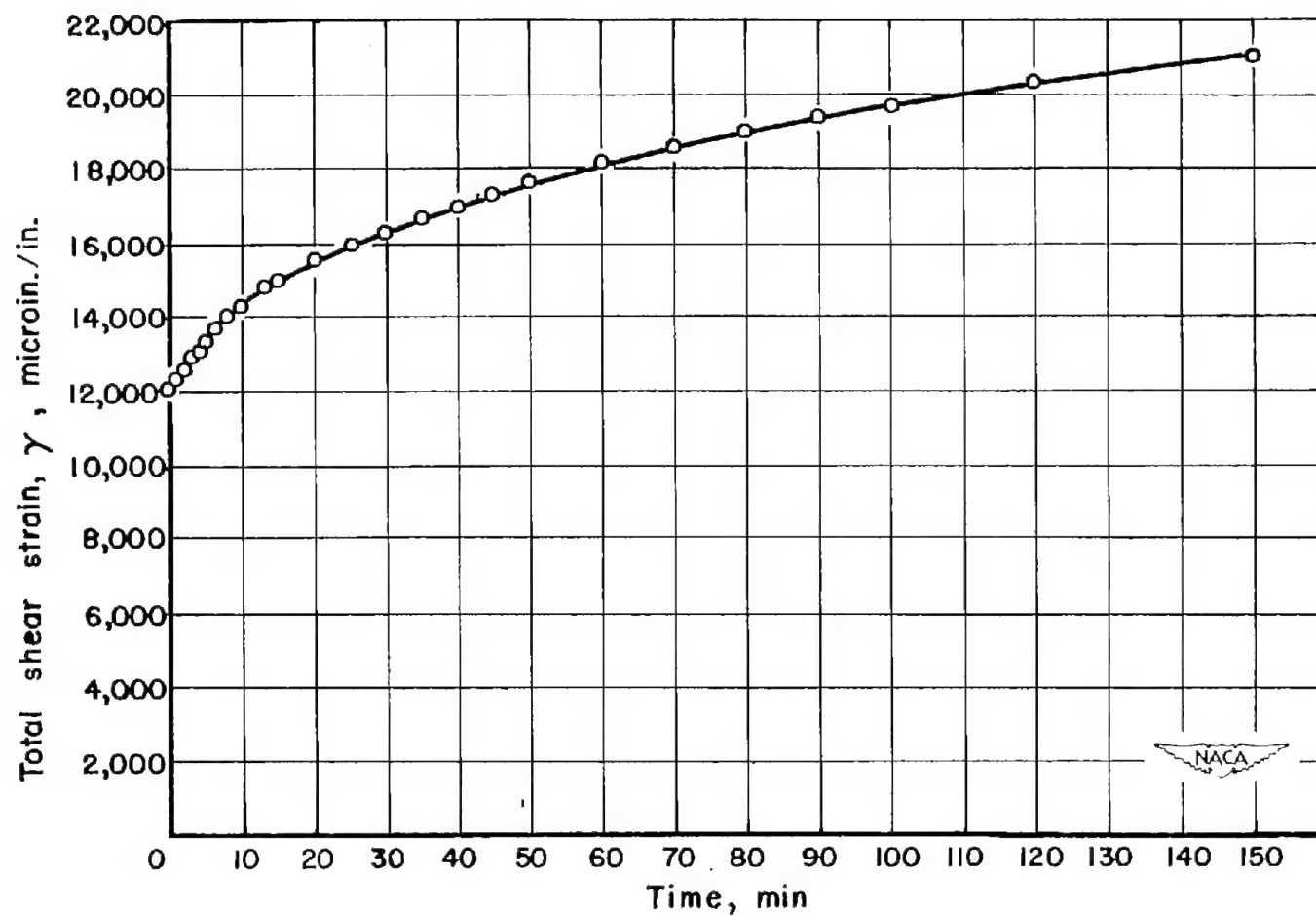


Figure 11.- Strain-time curve for crystal P-124 at 300° F with  $\tau = 300$  psi.

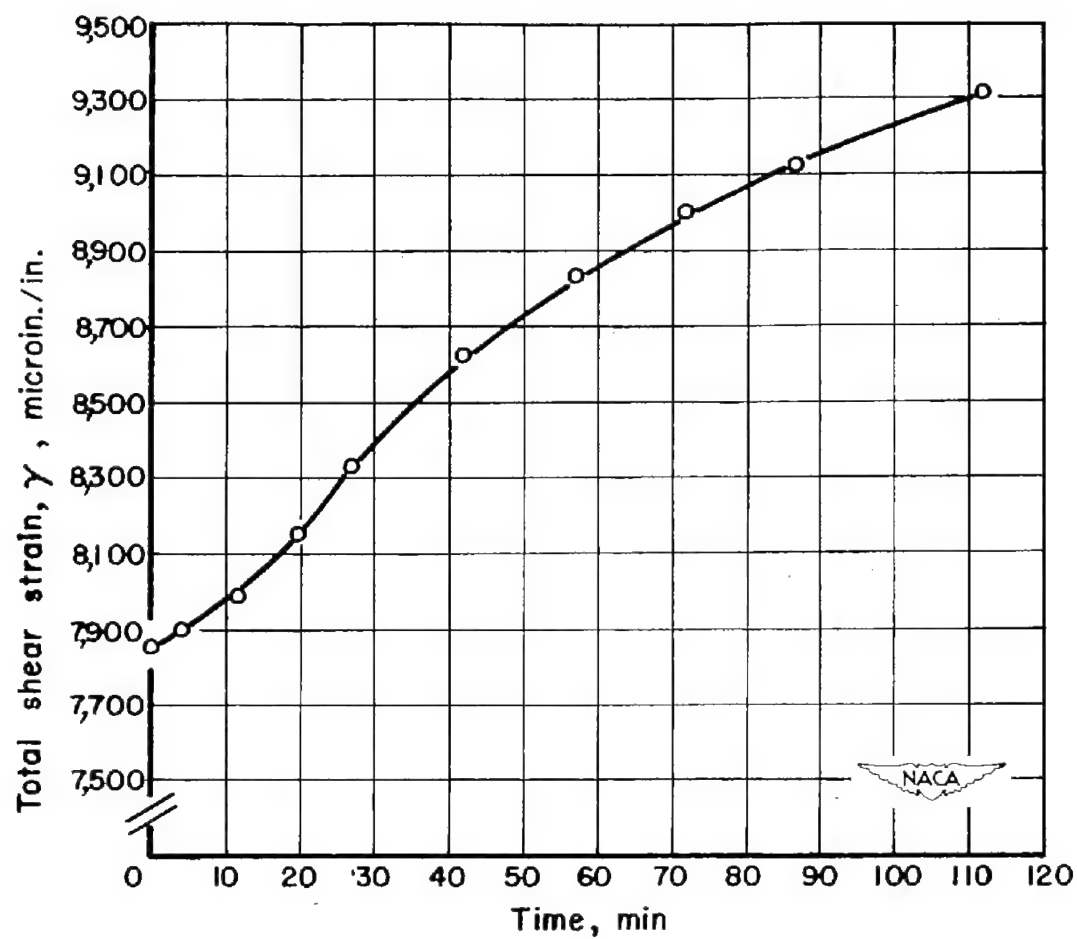


Figure 12.- S-shaped strain-time curve for crystal P-115 at 200° F with  $\tau = 300$  psi.

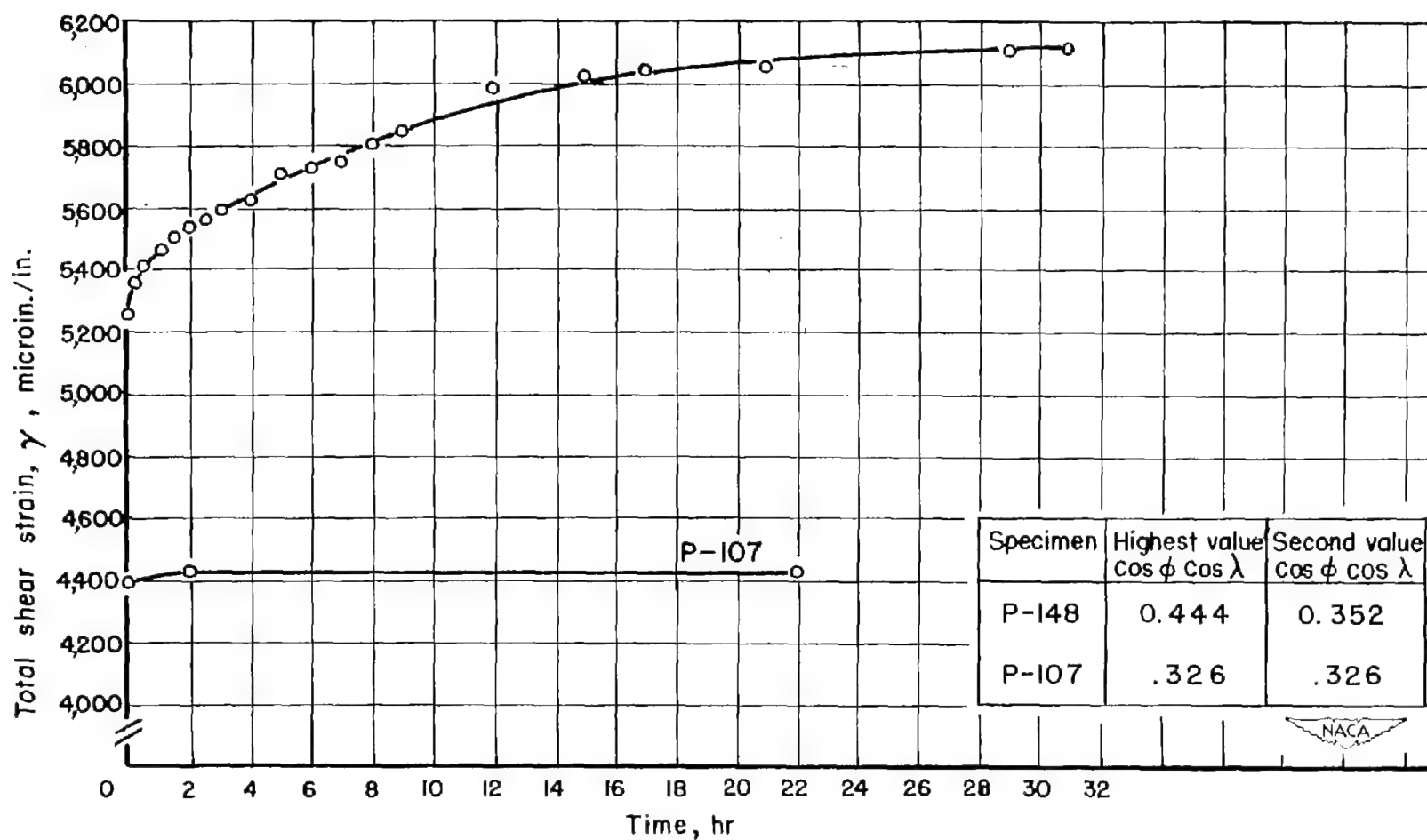


Figure 13.- Effect of duplex slip on strain-time curve of aluminum single crystals at 200° F with  $\tau = 200$  psi.

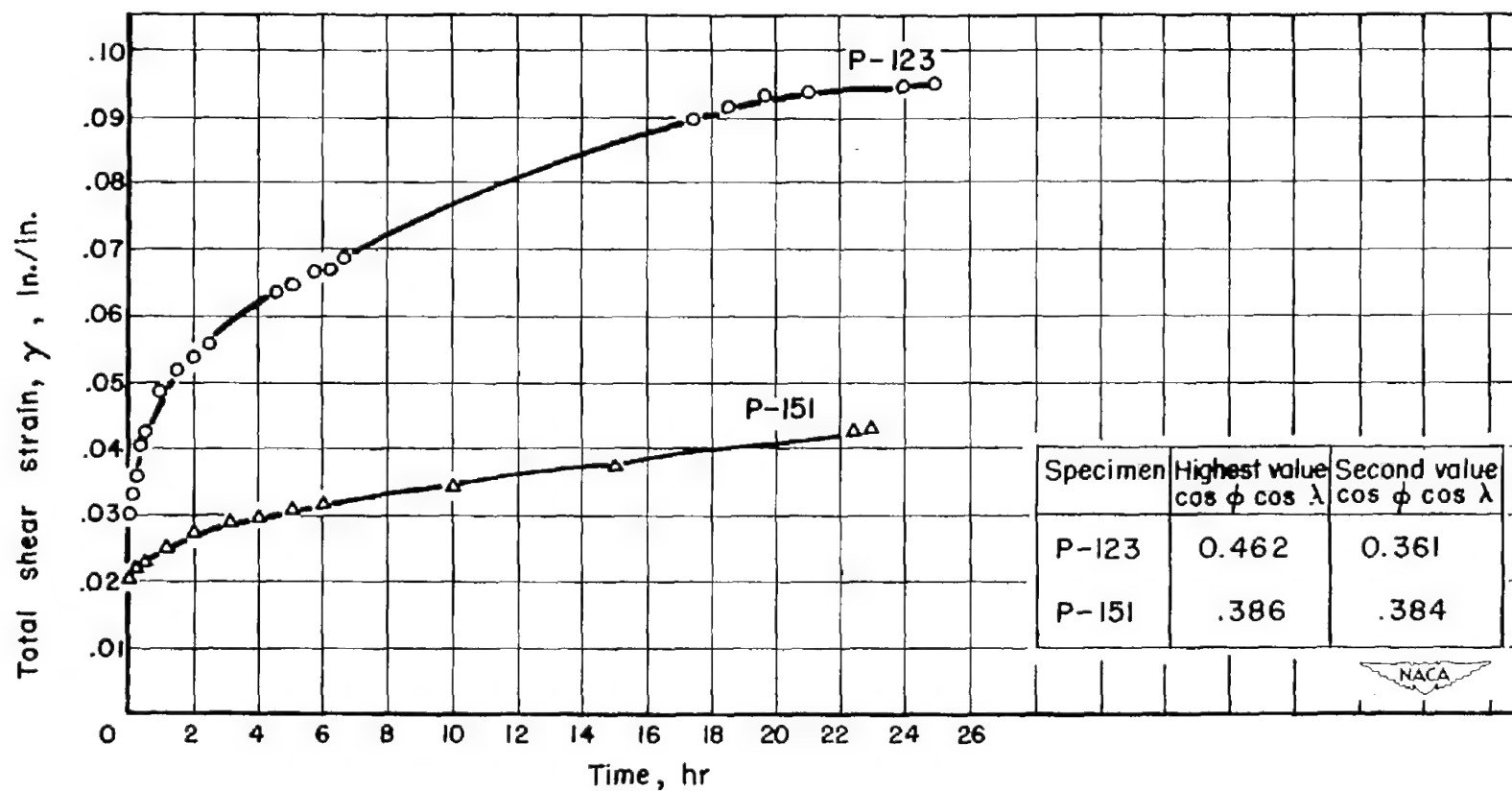


Figure 14.- Effect of duplex slip on strain-time curve of aluminum single crystals at 300° F with  $\tau = 400$  psi.



(a) Specimen P-115; test, 300-psi resolved shear stress at 200° F; surface, chemically polished; total extension, 0.6 percent.

(b) Specimen P-124; test, 300-psi resolved shear stress at 300° F; surface, etched; total extension, 2.5 percent.

Figure 15.- Strain markings from creep specimens. X400.



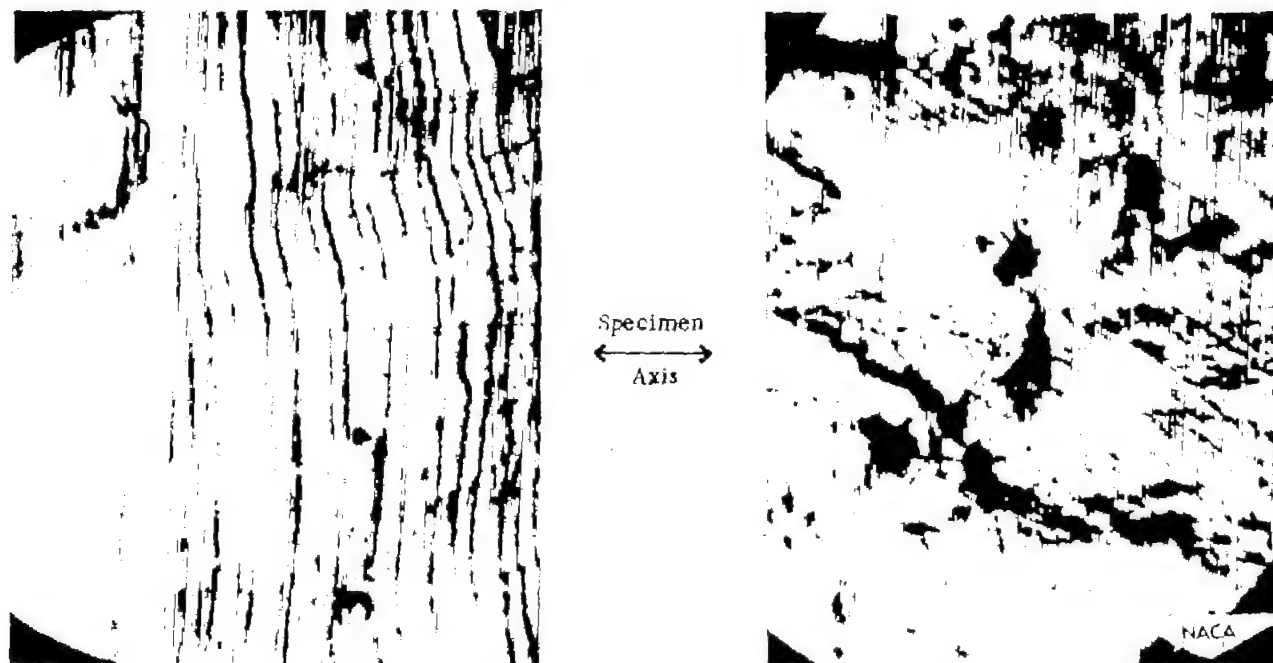
(c) Specimen P-123; test, 400-psi resolved shear stress at 300° F; surface, etched; total extension, 6 percent.

Specimen  
↔  
Axis



(d) Specimen P-150; test, 400-psi resolved shear stress at 400° F; surface, chemically polished; total extension, 10 percent.

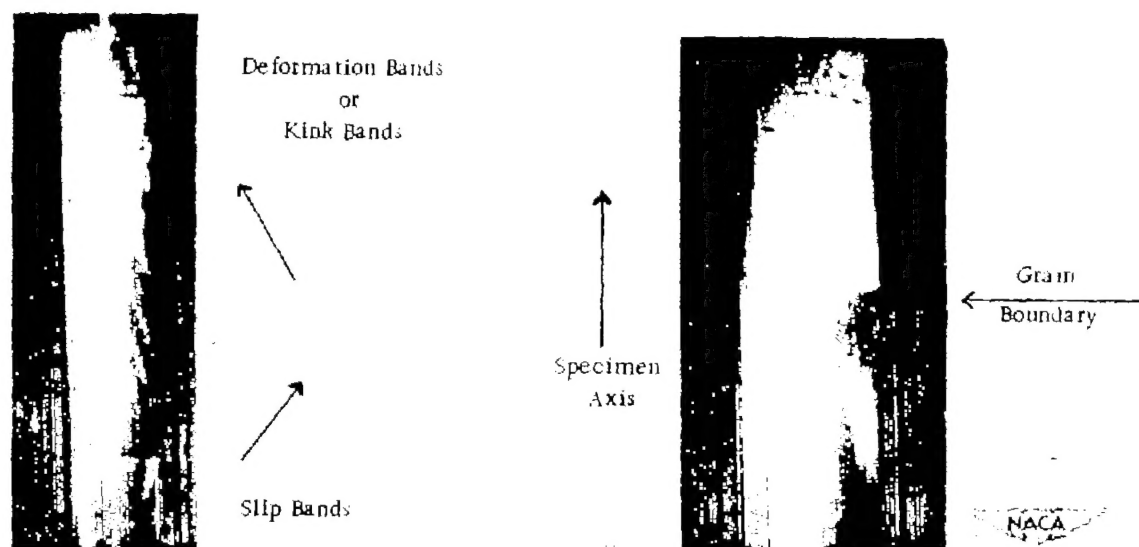
Figure 15.- Concluded.



(a) Specimen P-163; test, constant-load-rate at 200° F; surface, chemically polished; total extension, 18 percent; taken approximately parallel to  $\theta$ -direction of slip plane; X400.

(b) Specimen P-163; test, constant-load-rate at 200° F; surface, chemically polished; total extension, 18 percent; taken perpendicular to  $\theta$ -direction of slip plane; X400.

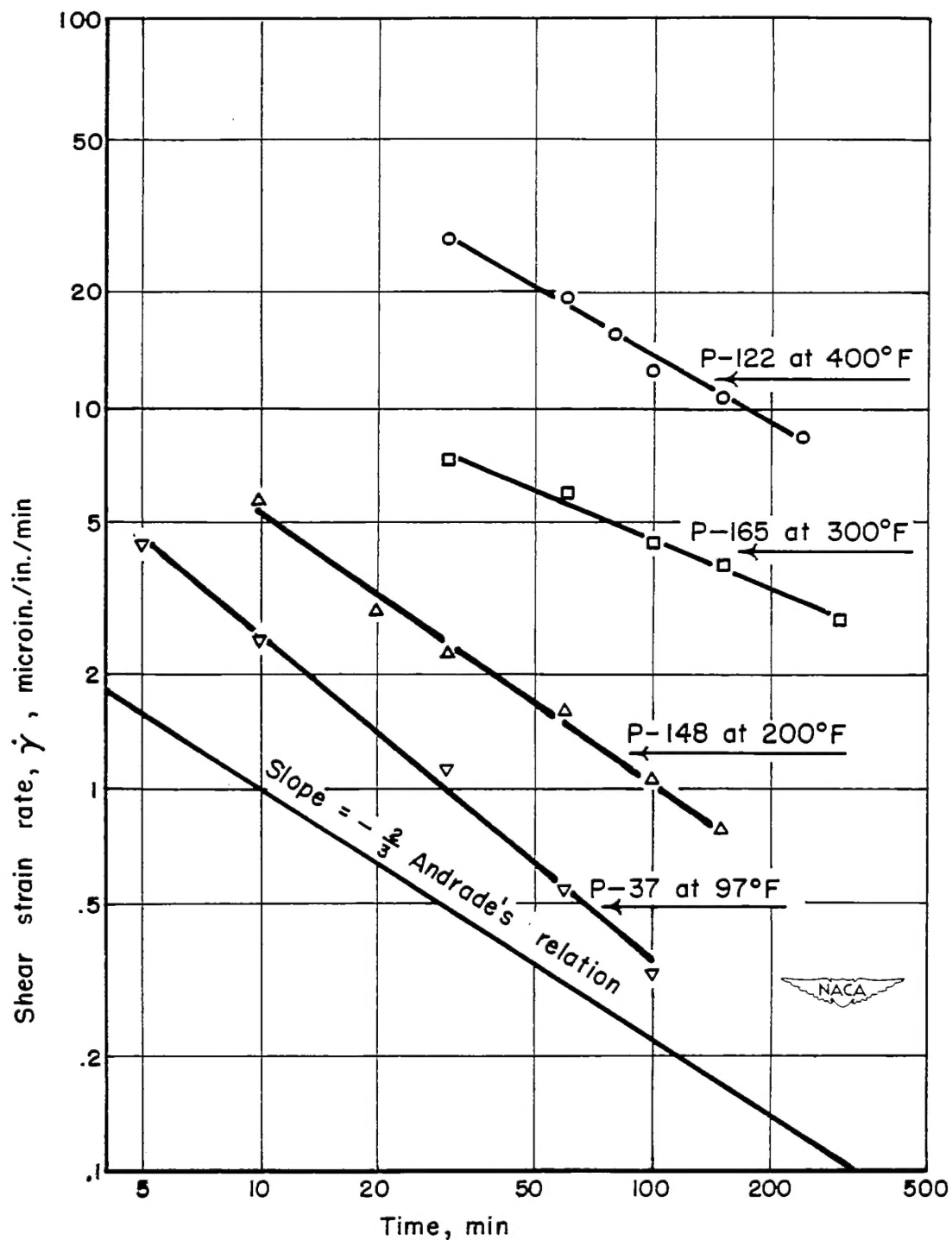
Figure 16.- Strain markings from tensile test and constant-load-rate test specimens.



(c) Specimen P-166; test, constant-load-rate at 200° F; surface, etched; total extension, 20 percent.

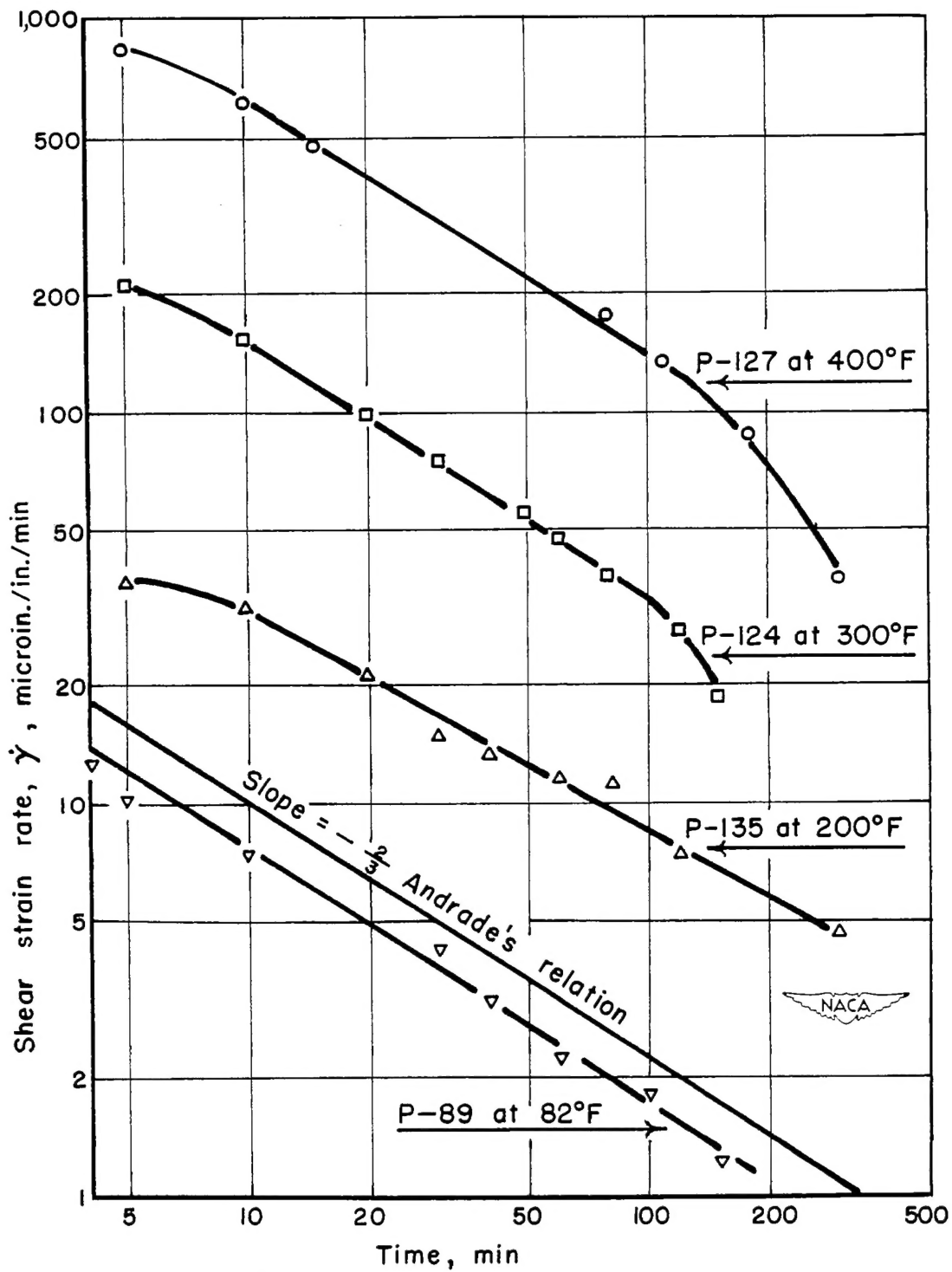
(d) Specimen P-161; test, tensile at 203° F; surface, etched; total extension, 17 percent.

Figure 16.- Concluded.



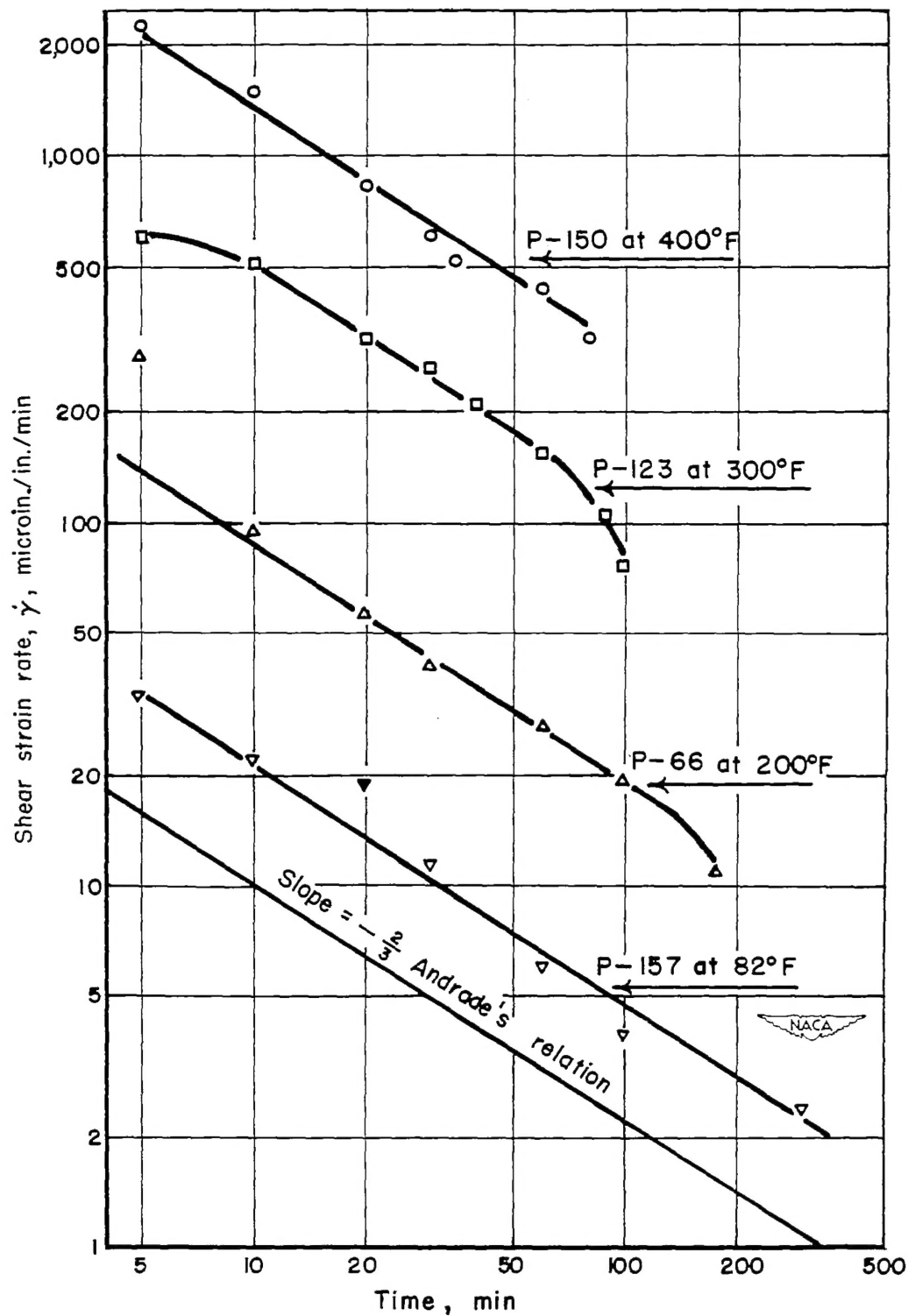
(a) 200-psi resolved shear stress.

Figure 17.- Creep of single crystals of aluminum at different values of resolved shear stress. Evaluation of Andrade's relation.



(b) 300-psi resolved shear stress.

Figure 17.- Continued.



(c) 400-psi resolved shear stress.

Figure 17.- Concluded.